**Figure 4.** Results of serum titer ELISA of antisera collected from ECL-antigens-immunized mice at one week before immunization (●) and one week after 5th immunization (■) to determine the immunogenicity of designed antigens. The titers were evaluated based on binding to each corresponding monomer peptide; (A) antiserum against C1 tetramer; (B) antiserum against L1 tetramer, (C) antiserum against C2 tetramer, and (D) antiserum against L2 tetramer. The antibody response was elicited in a representative mouse among four mice used for experiments.
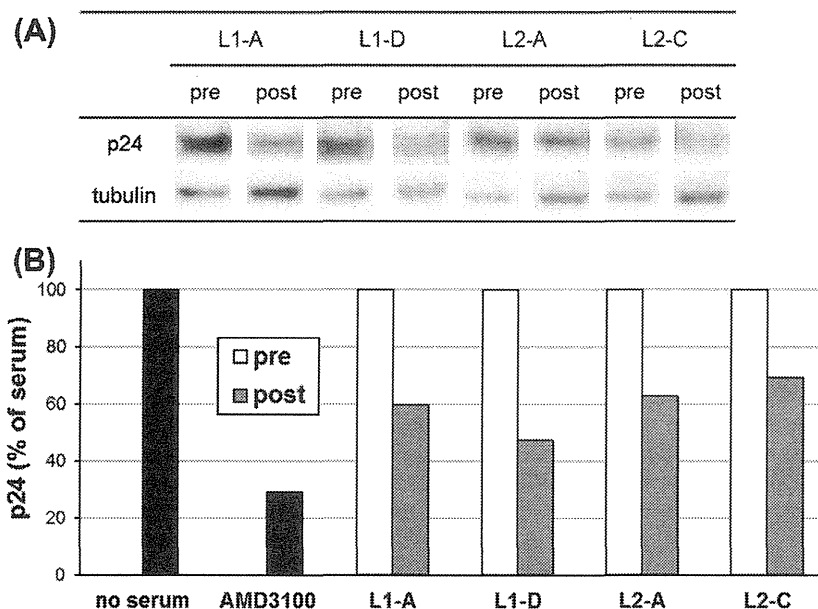
Figure 5. Results of a p24 assay using antisera collected from mice immunized with L1 and L2. (A) Two (L1-A and L1-D) of four (L1-A–D) suppressed p24 production, and two (L2-A and L2-C) of four (L2-A–L2-D) suppressed p24 production. (B) The average percentages of p24 production were calculated from the band intensities in panel A. Black bars are the data of experiments with no serum and with CXCR4 antagonist AMD3100 (1 μM). White Bars are the data of pre-immunization sera, and gray bars are the data of post-immunization sera, which were standardized based on the signals of tubulin. The statistical analyses are shown in Supplementary data.

assays utilizing the antisera bled from four mice for each antigen molecule. Two (L1-A, L1-D) of four (L1-A–L1-D) antisera produced in mice immunized with linear peptide L1 largely suppressed p24 production in comparison to pre-immunization sera (Fig. 5A). Two (L2-A, L2-C) of four (L2-A–L2-D) antisera produced in mice immunized with linear peptide L2 also largely suppressed p24 production compared to pre-immunization sera (Fig. 5A). The average percentages of p24 production were calculated from the intensities

of the bands in panel A of Figure 5 (Fig. 5B). Anti-C1 and anti-C2 antibodies were produced but had no significant anti-HIV-1 activity. Possible reasons for this result are (i) the antibody titer levels of L1- and L2-induced sera are higher than that of C1- and C2-induced sera, and (ii) the region around the site of conjugation between C1/C2 and MAPs might behave as an effective epitope for inhibition of HIV-1 entry. In murine serum, several peptides and proteins, for example an antimicrobial peptide α-defensin,[41] have been

reported to have inhibitory activity against HIV-1 entry. The antisera collected at both pre-immunization and post-immunization phases may contain α-defensin, which may affect their HIV-1 inhibitory activity. In this assay, the difference between the antisera collected at both pre-immunization and post-immunization phases was evaluated.

The Env glycoprotein gp120 is known to be highly glycosylated, and its mutation allows the escape of HIV-1 from neutralization by antibodies.[42] However, several antibodies isolated from sera of an African donor such as PG9, PG16[43,44] and VRC01[45] show broad and potent neutralizing activity as a result of recognition of the steric structure of gp120. These antibodies can neutralize 70–80% of HIV-1 strains isolated across all clades with potency approximately one order of magnitude higher than that reported previously for broadly neutralizing monoclonal antibodies. These results suggest that there may be antibody production mechanisms which recognize epitope structures and the development of antigen molecules designed to induce structure-specific antibodies are required.[46,47] We previously synthesized antigen molecules N36 trimer mimic[48] and C34 trimer mimic, based on highly conserved regions of gp41.[49,50] Mice were immunized with each antigen, and anti-HIV-1 antibodies that recognized tertiary structures of each antigen were induced. Antibodies induced by the immunization of CXCR4-ED-derived antigen molecules may have less potent anti-HIV-1 activity than broadly neutralizing antibodies PG9, PG16 and VRC01. They bind to the quaternary neutralizing epitopes on gp120,[51] in contrast, anti-CXCR4-ED antibodies have no time and space barriers in the binding to CXCR4. The tip of the V3 loop is only 30 Å from the target cell membrane[52] and blocking the CXCR4-ED may be more efficient than blocking the V3 loop. Therefore, antigen molecules which can effectively induce anti-CCR5/CXCR4 antibodies might have promise as AIDS vaccines.

3. Conclusion

The HIV-1 co-receptor CXCR4 is an attractive drug target with which to overcome the mutability of HIV-1. In this study, the CXCR4-ED-derived peptides, excluding ECL3, were conjugated with MAPs to produce antigen molecules. Only N1-derived antigen (N1 tetramer) was produced using SPAAC between an N1 dimer bearing azide moiety and a diyne. With the exception of N2 and N3, the CXCR4-ED-derived antigen molecules significantly induced antibodies against each corresponding antigen molecule but only the antisera induced by immunization of the linear peptides based on ECL1 and ECL2 (L1 and L2) exhibited HIV-1 inhibitory activity. The design of antigen molecules mimicking the flexible structure of proteins such as CXCR4-ED is difficult owing to lack of structural information. The X-ray crystal structures of the complexes of CXCR4 with ligands have been reported,[53] but the ligand-free structure has not been published. The results of the present and a previous[30] study suggested that the rational design of the cyclic peptides based on ECL1/ECL2 is possible, but data supporting the rational design of ECL-derived cyclic peptides with MAPs is unavailable. It is clear that, to develop more effective ECL-derived antigen molecules, the length of the linkers on MAPs should be optimized to avoid steric hindrance. This study has provided promising examples for the design of AIDS vaccines targeting the human protein CXCR4 to overcome mutability of HIV-1.

4. Experimental

4.1. Synthesis of the MAPs

The 2-branched azide template and the ClCH$_2$CO-GABA MAP were synthesized on a Rink amide resin (0.74 mmol/g, or

0.6 mmol/g) and the ClCH$_2$CO-(GABA)$_2$ MAP and BrCH$_2$CO-(GABA)$_2$ MAP were synthesized on a NovaSyn® TGR resin (0.21 mmol/g) by standard Fmoc-SPPS with Fmoc-Lys(Fmoc)-OH in the branch position. The constructed peptide was treated with 40 equiv of monochloroacetic acid or monobromoacetic acid, 40 equiv of DIPCI and 40 equiv of HOBt·H$_2$O for 1 h. Cleavage of peptides from resins and side chain deprotection were carried out by stirring for 1.5 h with a mixture of TFA, thioanisole, H$_2$O, m-cresol and TIS (10/0.75/0.5/0.25/0.1, v/v, 10 mL).

The 2-branched azide template for the conjugation of N1 was synthesized on a Rink amide resin (0.74 mmol/g, 0.05 mmol scale). The product (24.3 mg, 48% yield) was purified by preparative HPLC and characterized by ESI-TOF-MS: m/z calcd for C$_{35}$H$_{60}$Cl$_2$N$_{14}$O$_{10}$ [M+H]$^+$ 907.41, found 907.40.

The ClCH$_2$CO-GABA MAP for the conjugation of N2/N3 was synthesized on a Rink amide resin (0.60 mmol/g, 0.10 mmol scale). The product (93.8 mg, 45%) was purified by preparative HPLC and characterized by ESI-TOF-MS: m/z calcd for C$_{70}$H$_{121}$Cl$_4$N$_{23}$O$_{20}$ [M+H]$^+$ 1743.79, found 1746.23.

The ClCH$_2$CO-(GABA)$_2$ MAP for the conjugation of C1/L1 was synthesized on a NovaSyn® TGR resin (0.21 mmol/g, 0.10 mmol scale). The product (90.5 mg, 37%) was purified by preparative HPLC and characterized by ESI-TOF-MS: m/z calcd for C$_{86}$H$_{150}$Cl$_4$N$_{27}$O$_{24}$ [M+H]$^+$ 2085.01, found 2086.56.

The BrCH$_2$CO-(GABA)$_2$ MAP for the conjugation of C2/L2 was synthesized on a NovaSyn® TGR resin (0.21 mmol/g, 0.10 mmol scale). The product (56.2 mg, 22%) was purified by preparative HPLC and characterized by ESI-TOF-MS: m/z calcd for C$_{86}$H$_{150}$Br$_4$N$_{27}$O$_{24}$ [M+H]$^+$ 2260.81, found 2262.87.

4.2. Synthesis of N1 tetramer

N1 (20.7 mg, 7.88 μmol), the 2-branched azide template (4.03 mg, 3.95 μmol), and KI (22.8 mg, 137 μmol) were dissolved in 0.1 M sodium phosphate buffer at pH 7.8 (2 mL) under N$_2$. After stirring overnight at room temperature, the N1 dimer product (8.89 mg, 36%) was purified by preparative HPLC and characterized by ESI-TOF-MS: m/z calcd for C$_{237}$H$_{370}$N$_{70}$O$_{92}$S$_6$ [M+H]$^+$ 5862.52, found 5862.57.

sym-Dibenzo-1,5-cyclooctadiene-3,7-diyne[37] (0.0620 mg, 0.310 μmol) in dry MeOH (55.1 μL) was added to the N1 dimer containing an azide moiety (4.80 mg, 0.760 μmol) in dry MeOH (800 μL). After stirring overnight at room temperature under N$_2$, the N1 tetramer ligation product (1.38 mg, 36%) was purified by semipreparative HPLC and characterized by ESI-TOF-MS: m/z calcd. for C$_{490}$H$_{748}$N$_{140}$O$_{184}$S$_{12}$ [M+H]$^+$ 11925.02, found 11928.58.

4.3. Synthesis of N2 and N3 tetramers

N2 (21.2 mg, 7.03 μmol) and ClCH$_2$CO-GABA MAP (1.55 mg, 0.745 μmol) were dissolved in 0.1 M sodium phosphate buffer pH 7.8 (2 mL). After stirring overnight at room temperature under N$_2$, the N2 tetramer ligation product (6.77 mg, 65%) was purified by preparative HPLC and characterized by ESI-TOF-MS: m/z calcd for C$_{506}$H$_{769}$N$_{147}$O$_{184}$S$_{12}$ [M+H]$^+$ 12236.31, found 12237.32.

N3 (19.5 mg, 6.31 μmol) and ClCH$_2$CO-GABA MAP (1.64 mg, 0.790 μmol)) were dissolved in 0.1 M sodium phosphate buffer pH 7.8 (2 mL). After stirring overnight at room temperature under N$_2$, the N3 tetramer ligation product (5.82 mg, 52%) was purified by preparative HPLC and characterized by ESI-TOF-MS: m/z calcd for C$_{518}$H$_{801}$N$_{155}$O$_{168}$S$_8$ [M+H]$^+$ 12140.79, found 12140.97.

4.4. Synthesis of C1 and L1 tetramers

C1 (25.8 mg, 7.44 μmol) and ClCH$_2$CO-(GABA)$_2$ MAP (4.5 mg, 1.86 μmol) were dissolved in a 3:2 mixture (3.0 mL) of 0.1 M

sodium phosphate buffer pH 7.8 (containing 5.0 mM ethylenediaminetetraacetic acid; EDTA) and CH_3CN. After stirring overnight at room temperature under N_2, the C1 tetramer ligation product (5.31 mg, 18%) was purified by preparative HPLC and characterized by ESI-TOF-MS: m/z calcd for $C_{590}H_{902}N_{187}O_{168}S_8$ [M+H]$^+$ 13550.58, found 13553.77.

L1 (20.0 mg, 5.93 µmol) and $ClCH_2CO-(GABA)_2$ MAP (2.0 mg, 0.83 µmol) were dissolved in a 3:2 mixture (3.0 mL) of 0.1 M sodium phosphate buffer at pH 7.8 (containing 5.0 mM EDTA) and CH_3CN. After stirring overnight at room temperature under N_2, the L1 tetramer ligation product (5.06 mg, 40%) was purified by preparative HPLC and characterized by ESI-TOF-MS: m/z calcd for $C_{578}H_{890}N_{183}O_{164}S_4$ [M+H]$^+$ 13146.58, found 13150.70.

4.5. Synthesis of C2 and L2 tetramers

C2 (10.5 mg, 2.5 µmol) and $BrCH_2CO-(GABA)_2$ MAP (1.0 mg, 0.41 µmol) were dissolved in a 3:2 mixture (1.0 mL) of 0.1 M sodium phosphate buffer at pH 7.2 (containing 5.0 mM EDTA) and DMF. After stirring overnight at room temperature under N_2, the mixed C2 trimer and tetramer ligation products (tetramer 0.44 mg; trimer 0.36 mg, total yield 8%) were purified by preparative HPLC and characterized by ESI-TOF-MS; tetramer: m/z calcdfor $C_{778}H_{1122}N_{219}O_{224}S_4$ [M+H]$^+$ 17256.30, found 17263.79; trimer: m/z calcd for $C_{605}H_{883}N_{171}O_{175}NaS_3$ [M+Na]$^+$ 13468.50, found 13469.10.

L2 (56 mg, 13.2 µmol) and $BrCH_2CO-(GABA)_2$ MAP (4.0 mg, 1.53 µmol) were dissolved and stirred in the same manner as in the synthesis of the C2 tetramer. The mixed L2 trimer; tetramer ligation products (tetramer 7.18 mg and trimer 1.79 mg, total yield 32%) were purified by preparative HPLC and characterized by ESI-TOF-MS; tetramer: m/z calcd for $C_{786}H_{1154}N_{223}O_{228}S_4$ [M+H]$^+$ 17492.46, found 17497.33; trimer: m/z calcd for $C_{611}H_{904}N_{174}O_{178}S_3$ [M+H]$^+$ 13622.63, found 13626.37.

4.6. Immunization

Five-week-old male Balb/C mice, purchased from CLEA Japan, Inc. (Tokyo, Japan), were maintained in an animal facility under specific pathogen-free conditions. The experimental protocol used was approved by the ethical review committee of Tokyo Medical and Dental University. Freund's incomplete adjuvant and PBS were purchased from Wako Pure Chemical Industries (Osaka, Japan), DMSO (endotoxin free) was purchased from Sigma–Aldrich (St. Louis, MO).

All mice were habituated for one week and all six-week-old mice were bled one week before immunization. Antigen molecule (100 µg) was dissolved in DMSO (1 µL) and PBS (49 µL). This solution was mixed with Freund's incomplete adjuvant (50 µL) and the mixture was injected subcutaneously under anesthesia on days 0, 7, 14, 21 and 28. Four mice for each immunization were bled on days 5, 12, 19, 26 and 33. Serum was separated by centrifugation (1500 rpm) at 4 °C for 10 min, and inactivated at 56 °C for 30 min. Sera were stored at −80 °C before use.

4.7. ELISA assay

Tween-20 (polyoxyethylene (20) sorbitan monolaurate) and H_2O_2 (30%) were purchased from Wako. ABTS (2,2-azino-bis(3-ethylbenzothiazoline-6-sulfonic acid)diammonium salt) was purchased from Sigma–Aldrich. Anti-mouse IgG (H+L)(goat)-HRP was purchased from EMD Chemicals (San Diego, CA). Ninety six-well microplates were coated with 25 µL of a synthetic peptide at 10 µg/mL in PBS at 4 °C overnight. The coated plates were washed 10 times with distilled water and blocked with 150 µL of blocking buffer (0.02% PBST, PBS with 0.02% Tween 20, containing 5% skim milk) at 37 °C for 1 h. The plates were washed 10 times with distilled water. Mice sera were diluted in binding buffer (0.02% PBST with 1% skim milk), and 50 µL of twofold serial dilutions of sera from 1/10 to 1/1280 were added to the wells and allowed to incubate at 37 °C for 2 h. The plates were washed 10 times with distilled water. Twenty-five microliters of HRP-conjugated anti-mouse IgG, diluted 1:2000 in 0.02% PBST, was added to each well. After 45 min incubation, the plates were washed 10 times with distilled water and 25 µL of HRP substrate, prepared by dissolving 10 mg ABTS in 200 µL of HRP staining buffer—a mixture of 0.5 M citrate buffer (pH 4.0, 1 mL), H_2O_2 (3 µL), and H_2O (8.8 mL)—was added. After 30 min incubation, the reaction was stopped by addition of 25 µL/well 0.5 M H_2SO_4, and optical densities were measured at 405 nm.

4.8. Anti-HIV-1 assay (p24 assay)

The experiments using HIV-1 were performed in the biosafety level 3 laboratory #5 at the National Institute of Infectious Diseases. For virus preparation, 293T cells in a 60 mm dish were transfected with 10 µg of the pNL4-3 construct by the calcium phosphate method. The supernatant was collected 48 h after transfection, passed through a 0.45 µm filter, and stored at −80 °C as the virus stock.

For the viral neutralizing assay, MT-4 cells (1 × 10^5 cells/100 µL) were incubated in medium (100 µL) containing 10 µL of sera from immunized or pre-immunized mice for 1 h at 37 °C. The pretreated MT-4 cells were infected with HIV-1 NL4-3 (MOI = 0.05). At 3 days after infection, the virus-infected cells were collected and lysed with lysing buffer. The processed samples were subjected to SDS–PAGE to perform Western blotting. The HIV-1 gag p24 was detected with HIV-1 neutralizing serum (NIH AIDS Research and Reference Reagent Program).[54] The intensity of p24 bands was obtained by measuring their chemiluminescence and quantified using LAS-3000 (Fuji Film). The level of p24 in the culture supernatant was determined by the p24 ELISA kit (ZeptoMetrix Corporation).

Supplementary data

Supplementary data (HPLC charts of the synthetic compounds and HIV-1 inhibitory assay data (p24 Western)) associated with this article can be found, in the online version, at http://dx.doi.org/10.1016/j.bmc.2013.09.037.

References and notes

1. Barre-Sinoussi, F.; Chermann, J. C.; Rey, F.; Nugeyre, M. T.; Chamaret, S.; Gruest, J.; Dauguet, C.; Axler-Blin, C.; Vézinet-Brun, F.; Rouzioux, C.; Montagnier, L. Science 1983, 220, 878.
2. Melikyan, G. B.; Markosyan, R. M.; Hemmati, H.; Delmedico, M. K.; Lambert, D. M.; Cohen, F. S. J. Cell Biol. 2000, 151, 413.
3. Koyanagi, Y. Virus 2005, 55, 251.

4. Doranz, B. J.; Filion, L. G.; Diaz-Mitoma, F.; Sitar, D. S.; Sahai, J.; Baribaud, F.; Orsini, M. J.; Benovic, J. L.; Cameron, W.; Doms, R. W. AIDS Res. Hum. Retroviruses 2001, 17, 475.
5. Rizzuto, C. D.; Wyatt, R.; Hernandez-Ramos, N.; Sun, Y.; Kwong, P. D.; Hendrickson, W. A.; Sodroski, J. Science 1998, 280, 1949.
6. Chan, D. C.; Fass, D.; Berger, J. M.; Kim, P. S. Cell 1997, 89, 263.
7. Hashimoto, C.; Tanaka, T.; Narumi, T.; Nomura, W.; Tamamura, H. Expert Opin. Drug Discov. 2011, 6, 1067.
8. Berger, E. A.; Doms, R. W.; Fenyö, E. M.; Korber, B. T.; Littman, D. R.; Moore, J. P.; Sattentau, Q. J.; Schuitemaker, H.; Sodroski, J.; Weiss, R. A. Nature 1998, 391, 240.
9. Walker, D. K.; Abel, S.; Comby, P.; Muirhead, G. J.; Nedderman, A. N.; Smith, D. A. Drug Metab. Dispos. 2005, 33, 587.
10. Bogers, W. M.; Bergmeier, L. A.; Oostermeijer, H.; ten Haaft, P.; Wang, Y.; Kelly, C. G.; Singh, M.; Heeney, J. L.; Lehner, T. Vaccine 2004, 22, 2974.
11. Misumi, S.; Nakajima, R.; Takamune, N.; Shoji, S. J. Virol. 2001, 75, 11614.
12. Misumi, S.; Nakayama, D.; Kusaba, M.; Iiboshi, T.; Mukai, R.; Tachibana, K.; Nakasone, T.; Umeda, M.; Shibata, H.; Endo, M.; Takamune, N.; Shoji, S. J. Immunol. 2006, 176, 463.
13. Jacobson, J. M.; Thompson, M. A.; Lalezari, J. P.; Saag, M. S.; Zingman, P.; D'Ambrosio, B. S.; Stambler, N.; Rotshteyn, Y.; Marozsan, A. J.; Maddon, P. J.; Morris, S. A.; Olson, W. C. J. Infect. Dis. 2010, 201, 1481.
14. Jacobson, J. M.; Lalezari, J. P.; Thompson, M. A.; Fichtenbaum, C. J.; Saag, M. S.; Zingman, B. S.; D'Ambrosio, P.; Stambler, N.; Rotshteyn, Y.; Marozsan, A. J.; Maddon, P. J.; Morris, S. A.; Olson, W. C. Antimicrob. Agents Chemother. 2010, 54, 4137.
15. Jacobson, J. M.; Saag, M. S.; Thompson, M. A.; Fisch, M. A.; Liporace, R.; Reichman, R. C.; Redfield, R. R.; Fichtenbaum, C. J.; Zingman, B. S.; Patel, M. S.; Murga, J. D.; Pemrick, S. M.; D'Ambrosio, P.; Michael, M.; Kroger, H.; Ly, H.; Rotshteyn, Y.; Buice, R.; Morris, S. A.; Stavola, J. J.; Maddon, P. J.; Kremer, A. B.; Olson, W. C. J. Infect. Dis. 2008, 198, 1345.
16. Trkola, A.; Ketas, T. J.; Nagashima, K. A.; Zhao, L.; Cilliers, T.; Morris, L.; Moore, J. P.; Maddon, P. J.; Olson, W. C. J. Virol. 2001, 75, 579.
17. Tamamura, H.; Xu, Y.; Hattori, T.; Zhang, X.; Arakaki, R.; Kanbara, K.; Omagari, A.; Otaka, A.; Ibuka, T.; Yamamoto, N.; Nakashima, H.; Fujii, N. Biochem. Biophys. Res. Commun. 1998, 253, 877.
18. Fujii, N.; Oishi, S.; Hiramatsu, K.; Araki, T.; Ueda, S.; Tamamura, H.; Otaka, A.; Kusano, S.; Terakubo, S.; Nakashima, H.; Broach, J. A.; Trent, J. O.; Wang, Z. X.; Peiper, S. C. Angew. Chem., Int. Ed. 2003, 42, 3251.
19. DeClarcq, E.; Yamamoto, N.; Pauwels, R.; Balzarini, J.; Witvrouw, M.; De Vreese, K.; Debyser, Z.; Rosenwirth, B.; Peichl, P.; Datema, R. Antimicrob. Agents Chemother. 1994, 38, 668.
20. Schols, D.; Struyf, S.; Van Damme, J.; Este, J. A.; Henson, G.; DeClarcq, E. J. Exp. Med. 1997, 186, 1383.
21. Tamamura, H.; Ojida, A.; Ogawa, T.; Tsutsumi, H.; Masuno, H.; Nakashima, H.; Yamamoto, N.; Hamachi, I.; Fujii, N. J. Med. Chem. 2006, 49, 3412.
22. Tanaka, T.; Narumi, T.; Ozaki, T.; Sohma, A.; Ohashi, N.; Hashimoto, C.; Itotani, K.; Nomura, W.; Murakami, T.; Yamamoto, N.; Tamamura, H. ChemMedChem 2011, 6, 834.
23. Ichiyama, K.; Yokoyama-Kumakura, S.; Tanaka, Y.; Tanaka, R.; Hirose, K.; Nannai, K.; Edamatsu, T.; Yanaka, M.; Niitani, Y.; Miyano-Kurosaki, N.; Takaku, H.; Koyanagi, Y.; Yamamoto, N. Proc. Natl. Acad. Sci. U.S.A. 2003, 100, 4185.
24. Valks, G. C.; McRobbie, G.; Lewis, E. A.; Hubin, T. J.; Hunter, T. M.; Sadler, P. J.; Pannecouque, C.; De Clercq, E.; Archibald, S. J. J. Med. Chem. 2006, 49, 6162.
25. Khan, A.; Nicholson, G.; Greenman, J.; Madden, L.; McRobbie, G.; Pannecouque, C.; De Clercq, E.; Ullom, R.; Maples, D. L.; Maples, R. D.; Silversides, J. D.; Hubin, T. H.; Archibald, S. J. J. Am. Chem. Soc. 2009, 131, 3416.
26. Bridger, G. J.; Skerlj, R. T.; Hernandez-Abad, P. E.; Bogucki, D. E.; Wang, Z.; Zhou, Y.; Nan, S.; Boehringer, E. M.; Wilson, T.; Crawford, J.; Metz, M.; Hatse, S.; Princen, K.; De Clercq, E.; Schols, D. J. Med. Chem. 2010, 53, 1250.
27. Skerlj, R. T.; Bridger, G. J.; Kaller, A.; McEachern, E. J.; Crawford, J. B.; Zhou, Y.; Atsma, B.; Langille, J.; Nan, S.; Veale, D.; Wilson, T.; Harwig, C.; Haste, S.; Princen, K.; De Clercq, E.; Schols, D. J. Med. Chem. 2010, 53, 3376.
28. Narumi, T.; Tanaka, T.; Hashimoto, C.; Nomura, W.; Aikawa, H.; Sohma, A.; Itotani, K.; Kawamata, M.; Murakami, T.; Yamamoto, N.; Tamamura, H. Bioorg. Med. Chem. Lett. 2012, 22, 4169.
29. Narumi, T.; Aikawa, H.; Tanaka, T.; Hashimoto, C.; Ohashi, N.; Nomura, W.; Kobayakawa, T.; Takano, H.; Hirota, Y.; Murakami, T.; Yamamoto, N.; Tamamura, H. ChemMedChem 2013, 8, 118.
30. Hashimoto, C.; Nomura, W.; Narumi, T.; Fujino, M.; Tsutsumi, H.; Haseyama, M.; Yamamoto, N.; Murakami, T.; Tamamura, H. ChemMedChem 2013. Manuscript No. 201300289.
31. Letvin, N. L. Nat. Rev. Immunol. 2006, 6, 930.
32. Gaschen, B.; Taylor, J.; Yusim, K.; Foley, B.; Lang, D.; Novitsky, V.; Haynes, B.; Hahn, B. H.; Bhattacharya, T.; Korber, B. Science 2002, 296, 2354.
33. Garber, D. A.; Feinberg, M. B. AIDS Rev. 2003, 5, 131.
34. Tanaka, R.; Yoshida, A.; Murakami, T.; Baba, E.; Lichtenfeld, J.; Omori, T.; Kimura, T.; Tsurutani, N.; Fujii, N.; Wang, Z.; Peiper, S. C.; Yamamoto, N.; Tanaka, Y. J. Virol. 2001, 75, 11534.
35. Tam, J. P. Proc. Natl. Acad. Sci. U.S.A. 1988, 85, 5409.
36. Barnes, F. P.; Mehra, V.; Rivoire, B.; Fong, S. J.; Brennan, P. J.; Voegtline, M. S.; Minden, P.; Houghten, R. A.; Bloom, B. R.; Modlin, R. L. J. Immunol. 1992, 148, 1835.
37. Kii, I.; Shiraishi, A.; Hiramatsu, T.; Matsushita, T.; Uekusa, H.; Yoshida, S.; Yamamoto, M.; Kudo, A.; Hagiwara, M.; Hosoya, T. Org. Biomol. Chem. 2010, 8, 4051.
38. Werle, M.; Bernkop-Schnürch, A. Amino Acids 2006, 30, 351.
39. McGregor, D. P. Curr. Opin. Pharmacol. 2008, 8, 616.
40. Sato, A. K.; Viswanathan, M.; Kent, R. B.; Wood, C. R. Curr. Opin. Biotechnol. 2006, 17, 638.
41. Chang, T. L.; François, F.; Mosoian, A.; Klotman, M. E. J. Virol. 2003, 77, 6777.
42. Wei, X.; Decker, J. M.; Wang, S.; Hui, H.; Kappes, J. C.; Wu, X.; Salazar-Gonzales, J. F.; Salazar, M. G.; Kilby, J. M.; Saag, M. S.; Komarova, N. L.; Nowak, M. A.; Hahn, B. H.; Kwong, P. D.; Shaw, G. M. Nature 2003, 422, 307.
43. Walker, L. M.; Phogat, S. K.; Chan-Hui, P.; Wagner, D.; Phung, P.; Goss, J. L.; Wrin, T.; Simek, M. D.; Fling, S.; Mitcham, J. L.; Lehrman, J. K.; Priddy, F. H.; Olsen, O. A.; Frey, S. M.; Hammond, P. W.; Kaminsky, S.; Zamb, T.; Moyle, M.; Koff, W. C.; Poignard, P.; Burton, D. R. Science 2009, 326, 285.
44. McLellan, J. S.; Pancera, M.; Carrico, C.; Gorman, J.; Julien, J. P.; Khayat, R.; Louder, R.; Pejchal, R.; Sastry, M.; Dai, K.; O'Dell, S.; Patel, N.; Shahzad-ul-Hussan, S.; Yang, Y.; Zhang, B.; Zhou, T.; Zhu, J.; Boyington, J. C.; Chuang, G. Y.; Diwanji, D.; Georgiev, I.; Kwon, Y. D.; Lee, D.; Louder, M. K.; Moquin, S.; Schmidt, S. D.; Yang, Z. Y.; Bonsignori, M.; Crump, J. A.; Kapiga, S. H.; Sam, N. E.; Haynes, B. F.; Burton, D. R.; Koff, W. C.; Walker, L. M.; Phogat, S.; Wyatt, R.; Orwenyo, J.; Wang, L. X.; Arthos, J.; Bewley, C. A.; Mascola, J. R.; Nabel, G. J.; Schief, W. R.; Ward, A. B.; Wilson, I. A.; Kwong, P. D. Nature 2011, 480, 336.
45. Zhou, T.; Georgiev, I.; Wu, X.; Yang, Z.; Dai, K.; Finzi, A.; Kwon, T. D.; Scheid, J. F.; Shi, W.; Xu, L.; Yang, Y.; Zhu, J.; Nussenzweig, M. C.; Sodroski, J.; Shapiro, L.; Nabel, G. J.; Mascola, J. R.; Kwong, P. D. Science 2010, 329, 811.
46. Ofek, G.; Guenaga, F. J.; Schief, W. R.; Skinner, J.; Baker, D.; Wyatt, R.; Kwong, P. D. Proc. Natl. Acad. Sci. U.S.A. 2010, 107, 17880.
47. Burton, D. R. Proc. Natl. Acad. Sci. U.S.A. 2010, 107, 17859.
48. Nakahara, T.; Nomura, W.; Ohba, K.; Ohya, A.; Tanaka, T.; Hashimoto, C.; Narumi, T.; Murakami, T.; Yamamoto, N.; Tamamura, H. Bioconjugate Chem. 2010, 21, 709.
49. Nomura, W.; Hashimoto, C.; Ohya, A.; Miyauchi, K.; Urano, E.; Tanaka, T.; Narumi, T.; Nakahara, T.; Komano, J. A.; Yamamoto, N.; Tamamura, H. ChemMedChem 2012, 7, 205.
50. Hashimoto, C.; Nomura, W.; Ohya, A.; Urano, E.; Miyauchi, K.; Narumi, T.; Aikawa, H.; Komano, J. A.; Yamamoto, N.; Tamamura, H. Bioorg. Med. Chem. 2012, 20, 3287.
51. Euler, Z.; Bunnik, E. M.; Burger, J. A.; Boeser-Nunnink, B. D.; Grijsen, M. L.; Prins, J. M.; Schuitemaker, H. J. Virol. 2011, 85, 7236.
52. Huang, C. C.; Tang, M.; Zhang, M. Y.; Majeed, S.; Montabana, E.; Stanfield, R. L.; Dimitrov, D. S.; Korber, B.; Sodroski, J.; Wilson, I. A.; Wyatt, R.; Kwong, P. D. Science 2005, 310, 1025.
53. Wu, B.; Chien, E. Y. T.; Mol, C. D.; Fenalti, G.; Liu, W.; Katritch, V.; Abagyan, R.; Brooun, A.; Wells, P.; Bi, F. C.; Hamel, D. J.; Kuhn, P.; Handel, T. M.; Cherezov, V.; Stevens, R. C. Science 2010, 330, 1066.
54. Vujcic, L. K.; Quinnan, G. V., Jr. AIDS Res. Hum. Retroviruses 1995, 11, 783.

Anti-HIV-1 Peptide Derivatives Based on the HIV-1 Co-receptor CXCR4

Chie Hashimoto,[a] Wataru Nomura,[a] Tetsuo Narumi,[a] Masayuki Fujino,[b] Hiroshi Tsutsumi,[a] Masaki Haseyama,[a] Naoki Yamamoto,[b, c] Tsutomu Murakami,[b] and Hirokazu Tamamura*[a]

The human immunodeficiency virus type 1 (HIV-1) uses CD4 and the co-receptor CCR5 or CXCR4 in the process of cell entry. The negatively charged extracellular domains of CXCR4 (CXCR4-ED) interact with positive charges on the V3 loop of gp120, facilitating binding via electrostatic interactions. The presence of highly conserved positively charged residues in the V3 loop suggests that CXCR4-ED-derived inhibitors might be broadly effective inhibitors. Synthetic peptide derivatives were evaluated for anti-HIV-1 activity. The 39-mer extracellular N-terminal region (NT) was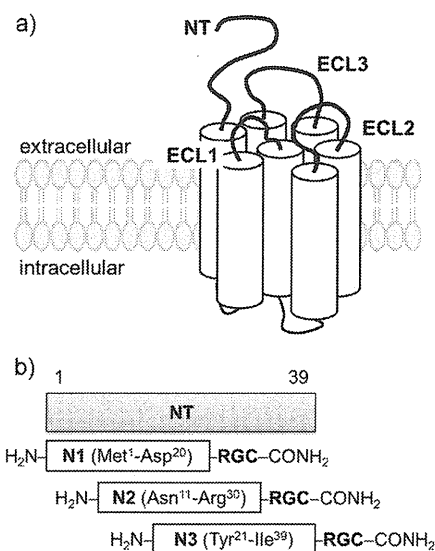 divided into three fragments with 10-mer overlapping sites (N1–N3), and these linear peptides were synthesized. Peptide N1 contains Met1–Asp20 and shows significant anti-HIV-1 activity. Extracellular loops 1 and 2 (ECL1 and 2) were mimicked by cyclic peptides C1 and C2, which were synthesized by chemoselective cyclization. Cyclic peptides C1 and C2 show higher anti-HIV-1 activity than their linear peptide counterparts, L1 and L2. The cytotoxicities of C1 and C2 are lower than those of L1 and L2. These results indicate that Met1–Asp20 segments of the NT and cyclic peptides of ECL1 and ECL2 are potent anti-HIV-1 drug candidates.

Introduction

Almost 30 years have passed since the human immunodeficiency virus (HIV) was discovered to be responsible for acquired immunodeficiency syndrome (AIDS).[1] Infection by HIV-1 is initiated by adsorption with the primary host cell receptor CD4[2] and the co-receptors CCR5 or CXCR4.[3–8] Initially, the HIV-1 envelope glycoprotein gp120 interacts with CD4, triggering conformational changes within gp120 that result in exposure of the co-receptor binding site, which is composed of the V3 loop and the gp120 bridging sheet.[3] To date, various CCR5/CXCR4 antagonists have been developed as anti-HIV-1 agents.[9] Maraviroc (4,4-difluoro-N-[(1S)-3-[(3-exo)-3-[3-methyl-5-(1-methylethyl)-4H-1,2,4-triazol-4-yl]-8-azabicyclo-[3.2.1]oct-8-yl]-1-phenylpropyl]cyclohexanecarboxamide) was the first CCR5 antagonist approved by the FDA.[10] A potent CXCR4 antagonist T140, a 14-mer cyclic peptide derived from polyphemusin II, was developed by our research group,[11] and a 5-mer cyclic peptide FC131 was developed by further modification of T140.[12] Small-molecule CXCR4 antagonists including AMD3100,[13,14] Dpa–zinc complex,[15] azamacrocyclic–zinc com-

plexes,[16] KRH-1636,[17] and other compounds[18–22] have been developed.

The HIV-1 co-receptors CCR5 and CXCR4 are classified as a member of the seven transmembrane G-protein-coupled receptor (7TMGPCR) family, and have an N-terminal extracellular region (NT) and three extracellular loops (ECL1–3) as the extracellular domains (ED) as shown in Figure 1a. CXCR4-ED has more negative charges than CCR5-ED, with net charges of 0 on the NT, −1 on ECL1, +5 on ECL2, and −1 on ECL3. CXCR4-ED has net charges of −6 on the NT, 0 on ECL1, −3 on ECL2, and

[a] Dr. C. Hashimoto, Dr. W. Nomura, Dr. T. Narumi, Dr. H. Tsutsumi,
    M. Haseyama, Prof. H. Tamamura
    Institute of Biomaterials and Bioengineering
    Tokyo Medical and Dental University
    2-3-10 Kandasurugadai, Chiyoda-ku, Tokyo 101-0062 (Japan)
    E-mail: tamamura.mr@tmd.ac.jp
[b] Dr. M. Fujino, Prof. N. Yamamoto, Dr. T. Murakami
    AIDS Research Center, National Institute of Infectious Diseases
    1-23-1 Toyama, Shinjuku-ku, Tokyo 162-8640 (Japan)
[c] Prof. N. Yamamoto
    Department of Microbiology, Yong Loo Lin School of Medicine
    National University of Singapore, Singapore 117597 (Singapore)

⌨ Supporting information for this article is available on the WWW under
    http://dx.doi.org/10.1002/cmdc.201300289.

Figure 1. a) Schematic view of a 7TMGPCR, CXCR4. The extracellular N-terminal region (NT) and extracellular loops 1-3 (ECL1–ECL3) are indicated. b) The 39-mer peptide NT was divided into three fragment peptides, N1–N3.

−1 on ECL3[23] and has electrostatic interactions with both its endogenous ligand CXCL12/SDF-1α[24] and the viral envelope protein gp120.[25–27] The negatively charged amino acid residues on CXCR4-ED are responsible for the binding of CXCL12/SDF-1α or gp120.

In the development of anti-HIV-1 drugs, viral mutation is the main obstacle, and it is therefore useful to target amino acid sequences that are conserved among various strains. The co-receptor binding site on the V3 loop is a variable region, but positively charged amino acid residues such as Arg3, Arg/Lys9–10, Arg13, Arg31, and His34 that are responsible for binding to CCR5/CXCR4 are highly conserved amongst various strains,[28–30] and these positively charged amino acid residues can be an appropriate target for the development of HIV-1 entry inhibitors. Herein, we focus on peptidic inhibitors that bind to the conserved basic residues on the V3 loop of gp120, which might suppress the emergence of resistant viruses. Peptide derivatives based on CXCR4-ED were synthesized and their anti-HIV-1 activities have been evaluated in a search for drug candidates which can neutralize a broad variety of HIV-1 strains.

Results and Discussion

Design

Acidic amino acid residues on the NT are thought to be important for the interaction between the V3 loop and CXCR4.[26,31] The co-crystal structure (Figure 3 below) of CXCR4 and a T140[11]-derived CXCR4 antagonist CVX15 or a small molecule CXCR4 antagonist IT1t, shows that nine or seven amino acid residues on or around ECL1 and ECL2 of CXCR4-ED have polar interactions with these CXCR4 antagonists, while only one amino acid residue on ECL3 interacts with each antagonist.[32] Consequently, in this study, peptides derived from the NT, ECL1, and ECL2, not but ECL3, were synthesized in an attempt to develop entry inhibitors. As the NT is a linear peptide and ECLs form loop architectures (Figure 1 a), linear fragment peptides of NT and cyclic peptides derived from ECL1 and ECL2 were synthesized (Figure 1 b). The Cys residues involved in two disulfide bonds in CXCR4, between Cys28 on the NT and Cys274 on ECL3, and between Cys109 on ECL1 and Cys186 on ECL2 were replaced by Ser to avoid disulfide formation and reaction with a carrier protein or peptide. The 39-mer NT was segmented into NT-fragment peptides: N1 (Met1–Asp20), N2 (Asn11–Arg30), and N3 (Tyr21–Ile39), retaining 10-mer overlapping sites. The tyrosine residues (Tyr7, Tyr12, and Tyr21) in the NT are post-translationally sulfated and are implicated in the reaction between CXCR4 and CXCL12/SDF-1α.[31,33,34] However, in the synthesis of

sulfo-Tyr-containing peptides, the conditions for the cleavage of the peptides from the resin must be carefully selected because sulfonyl groups are acid labile.[35] Accordingly, NT-fragment peptides in which Tyr is substituted for sulfo-Tyr were synthesized. On the C terminus of each NT-fragment peptide, three additional amino acid residues were attached; Arg as a hydrophilic amino acid residue, Gly as a spacer, and Cys as a ligation site for a carrier such as BSA, KLH, or multi-antigen peptides (MAP) so that the antigenicity of these peptides could be evaluated in future studies (Figure 1 b).

Two different types of cyclization strategies were used to synthesize cyclic peptides of ECL1 and ECL2 which mimic their loop architectures. A cyclic peptide based on ECL1 (C1) was designed with double repeats of Arg and Glu (RERE) at both the N and C termini to increase the aqueous solubility and to be cyclized by a reaction between the N-terminal chloroacetyl group and the C-terminal Cys thiol group in a dilute solution, pH 7.8 (Scheme 1). As in the NT-fragment peptides, another Cys residue was fused to the N terminus to create the ligation site with a carrier. Accordingly, an Fmoc-Cys(Acm)-OH was con-
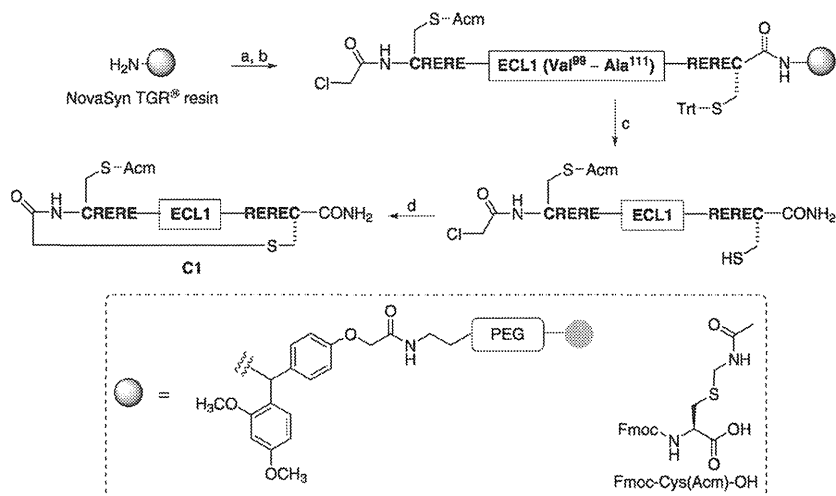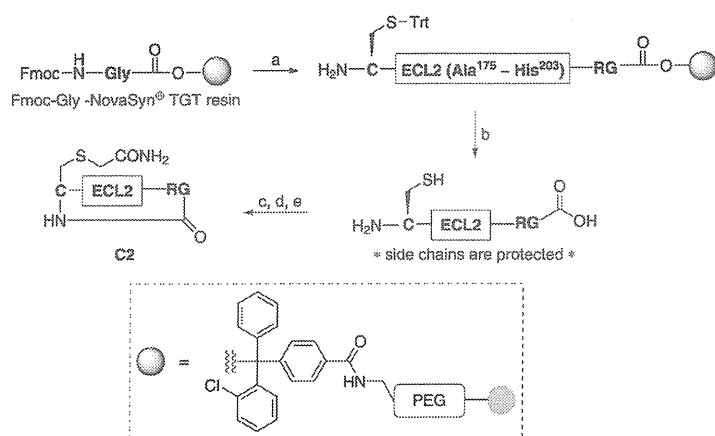

Scheme 1. Synthesis of a cyclic peptide of ECL1, C1. *Reagents and conditions*: a) Fmoc SPPS; b) 2-chloroacetic acid, HOBt·H₂O, DIPCI, DMF; c) TFA, thioanisole, *m*-cresol, EDT, H₂O, TIS; d) H₂O, CH₃CN, pH 7.8 adjusted with NH₃(aq).

densed at the N terminus, in which the Cys side chain was protected with an acetamidemethyl group (Acm) that can be cleaved with silver trifluoromethanesulfonate (AgOTf) in TFA, and an Fmoc-Cys(Trt)-OH was condensed at the C terminus to avoid reactions between the thiol group on the N-terminal Cys and the chloroacetyl group.

A cyclic peptide based on ECL2 (C2) could not be synthesized in this way (data not shown), and a different C2 variant was designed to cyclize in a head-to-tail cyclization using HOBt/HBTU/DIEA as shown in Scheme 2. The N-terminal Cys was fused as a ligation site with a carrier, and the C-terminal Arg was fused as a hydrophilic residue and the C-terminal Gly as a spacer.

Additionally, all peptides, with the exception of C1, were treated with iodoacetamide in 0.1 M sodium phosphate buffer

Scheme 2. Synthesis of a cyclic peptide of ECL2, C2. *Reagents and conditions*: a) Fmoc SPPS; b) AcOH, TFE, CH_2Cl_2; c) HOBt·H_2O, HBTU, DIPEA, DMF; d) TFA, thioanisole, *m*-cresol, EDT, H_2O, TIS; e) iodoacetamide, 0.1 M sodium phosphate buffer, pH 7.8.

The crude peptide was purified to obtain a cyclic peptide C1 as a colorless powder.

C2, a cyclic peptide based on ECL2, was synthesized on an Fmoc-Gly NovaSyn TGT resin. The synthetic peptide on the resin was treated with AcOH/TFE/CH_2Cl_2 to obtain the protected crude peptide, and this was followed by cyclization involving condensation of the N-terminal amino group with the C-terminal carboxyl group using HOBt/HBTU/DIEA. The side chains of the cyclic peptides were deprotected with TFA/thioanisole/*m*-cresol/EDT/TIS/H_2O and the crude peptides were purified by HPLC. Subsequently, the free thiol group on the N terminus was capped with iodoacetamide in 0.1 M sodium phosphate buffer at pH 7.8 to produce a cyclic peptide C2 as a colorless powder. Linear peptides of ECL1 (L1) and ECL2 (L2) were synthesized as controls for cyclic peptides C1 and C2 (Supporting Information figures 3 and 5). The amino acid sequences of thiol-capped CXCR4-ED-derived peptides are shown in Figure 2.

at pH 7.8 to cap thiol groups of Cys residues fused as ligation sites with a carrier (Figure 2). The thiol group of the N-terminal Cys on C1 is protected with Acm.

Peptide synthesis

All peptides were synthesized by standard Fmoc solid-phase peptide synthesis (SPPS) and characterized by ToF-ESIMS. The three NT-fragment peptides (N1–N3) containing 10-mer overlapping regions to facilitate investigation of active sites were synthesized on NovaSyn TGR resin. After HPLC purification, free thiol groups on the C terminus were capped with iodoacetamide in 0.1 M sodium phosphate buffer at pH 7.8, producing N1–N3 as colorless powders (Supporting Information figure 1).

C1, a cyclic peptide based on ECL1, was synthesized on a NovaSyn TGR resin, and then cleaved from the resin with a mixture of TFA/thioanisole/*m*-cresol/EDT/TIS/H_2O. After deprotection and cleavage from the resin, the C1 linear peptide was dissolved in a dilute solution of CH_3CN/H_2O, and the solution was adjusted to pH 7.8 with an aqueous ammonia solution.

Anti-HIV-1 activity

The anti-HIV-1 activity and cytotoxicity of the synthetic peptides were assessed by a 3-(4,5-dimethylthiazol-2-yl)-2,5-diphenyltetrazolium bromide (MTT) assay and the results are presented in Table 1. Of the synthetic peptides, N1 showed the highest anti-HIV-1 activity ($EC_{50} = 0.88$ μM), and did not show significant cytotoxicity at concentrations below 10 μM. N2 and N3 failed to show either significant anti-HIV-1 activity or cytotoxicity, indicating that N2 and N3 cannot bind to the V3 loop of gp120. The negatively charged amino acid residues of the extracellular domains of CXCR4 interact with the positively charged amino acid residues on the V3 loop of gp120. Of the peptides N1–N3, N1 has the greatest number of negative charges and it was hypothesized that it might bind strongly to the V3 loop and thus inhibit HIV-1 entry. The amino acid sequence of the fragment peptide N1 (Met 1–Asp 20) contains two sulfo-Tyr, Tyr 7 and Tyr 12 and sulfotyrosines on the NT of
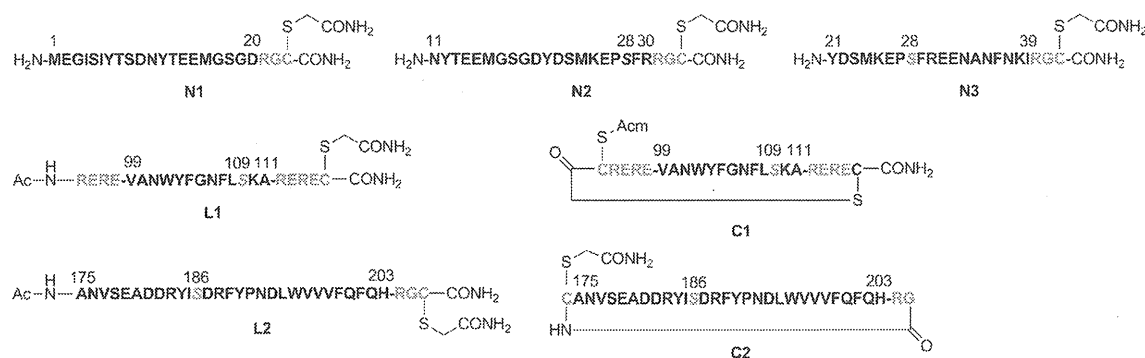
Figure 2. Structures of synthetic CXCR4-ED-derived peptides. L1 is a thiol-capped linear peptide of ECL1, C1 is a thiol-capped cyclic peptide of ECL1, L2 is a thiol-capped linear peptide of ECL2, and C2 is a thiol-capped cyclic peptide of ECL2. R and E (in grey) are Arg and Glu residues, respectively, added to increase solubility. C (in grey) is used as a ligation site with multi-antigen peptides (MAP). Cys 109 on ECL1 and Cys 186 on ECL2 were mutated to Ser (S, grey italics) to avoid reaction with MAP at these sites.

– 220 –

Table 1. Anti-HIV-1 activity and cytotoxicity of CXCR4-ED-derived peptides.[a]					
Compd	EC_{50} [µM]	CC_{50} [µM]	Compd	EC_{50} [µM]	CC_{50} [µM]
N1	0.88	>10	L1	50[b]	61
N2	>10	>10	L2	>25	35
N3	>10	>10	C1	35	>200
AMD3100	0.06	>20	C2	32	133
			AMD3100	0.096	18

[a] The number of viable cells was determined using the MTT method. A CXCR4 antagonist (AMD3100) was used as positive control. EC_{50} values are the concentrations resulting in 50% protection from HIV-1-induced cytopathogenicity in MT-4 cells. CC_{50} values are the concentrations required for a 50% decrease in MT-4 cell viability. All data are the mean values from three independent experiments. The data on the left and right columns are from two independent assays under identical conditions. [b] 48% inhibition.

CCR5 have been reported to be critical for specific binding to the V3 loop.[36] In contrast, the fragment peptide **N1** (Met 1–Asp 20), which has no sulfo-Tyr, has significant anti-HIV-1 activity. This result indicates that the NT of CCR5, with less negatively charged amino acid residues than that of CXCR4, might require sulfo-Tyr for the interaction between the NT and the V3 loop, because the sulfate groups bear a negative charge. Sulfo-Tyr residues on CXCR4-NT might be related to the interaction between CXCR4 and gp120, or an endogeneous ligand CXCL12/SDF-1α.[37,38] Sulfo-Tyr-containing peptides however are difficult to handle due to the sensitivity of sulfonyl groups to acidic conditions.[35] This makes sulfo-Tyr-containing peptides difficult to develop as drugs and **N1** might be a potent anti-HIV-1 drug candidate because it contains no sulfo-Tyr. The cytotoxicity of the NT-fragment peptides is minimal.

The cyclic peptides **C1** and **C2** are less cytotoxic and more potent than their corresponding linear peptides **L1** and **L2**. If ECL-derived peptides are to be developed as entry inhibitors, they might inhibit the interaction between CXCR4 and gp120 by their binding to the V3 loop of gp120. Cyclic peptides **C1** and **C2** were thought to bind to the V3 loop with higher binding affinity than linear peptides **L1** and **L2** indicating that **C1** and **C2** might be able to mimic the structures of native ECL1 and ECL2 effectively. Cyclization also affected the cytotoxicities of ECL-derived peptides. The cytotoxicity of **C1** and **C2** were lower than **L1** and **L2**. The V3 loop is thought to be composed of three regions: 1) the base of the loop containing a disulfide bond; 2) the stem, a conformationally flexible region; and 3) the tip, a conserved region (Figure 3a).[36,39] According to models of CXCR4 with gp120 by Wu et al., the NT of CXCR4-ED initially binds to the V3 base, and then the ligand-binding cavity, the V3 stem and tip bind to ECL2 and ECL3 (Figure 3a).[32] The NT can bind to the V3 base alone, however, amino acid residues related to the V3 stem and tip binding dot on sequentially discontinuous regions. This might explain why **N1** has potent anti-HIV-1 activity whereas **C1** and **C2** have only moderate anti-HIV-1 activity.
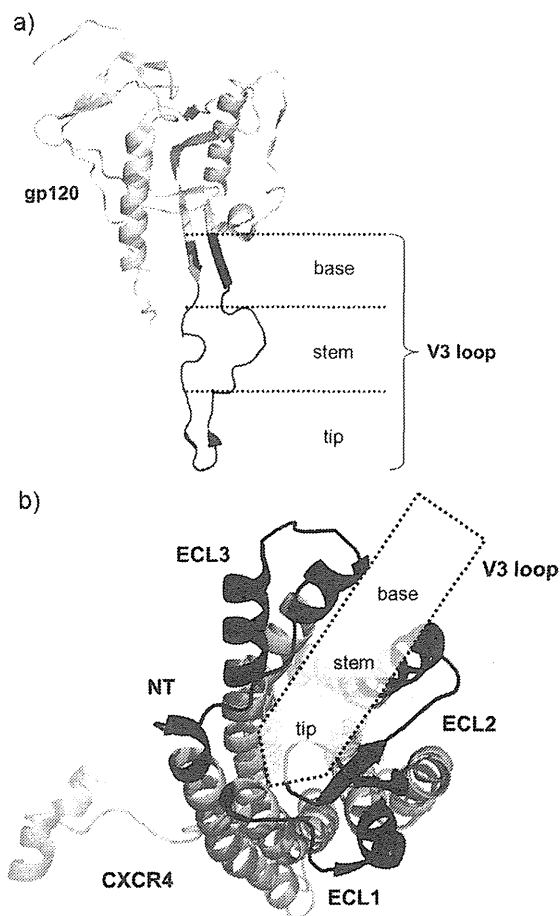
Figure 3. a) X-ray crystal structure of the gp120 V3 loop (PDB ID: 2B4C):[40] gp120 is depicted in light grey, and the section Lys 117–Gln 203 is hidden to show the V3 loop clearly. b) Predicted binding of CXCR4 (PDB ID: 3ODU)[32] and the V3 loop: the NT is indicated, and Met 1–Glu 26 is truncated because these residues with undefined density are presumed to be disordered. ECL1–3 are also indicated; Wu et al.[32] predicted that the V3 tip is inserted into the ligand binding pocket on CXCR4, the V3 base interacts with NT, and the V3 stem/tip interact with ECL1–3. These images were generated with PyMOL.[41]

Conclusions

Peptidic inhibitors focusing on electrostatic interactions between CXCR4 and the gp120 V3 loop of the HIV-1 envelope protein have been synthesized. Anti-HIV-1 agents targeting the V3 loop, whose basic amino acid residues are highly conserved among various strains, might have a significant advantage in suppressing the emergence of drug resistant viruses. The NT, ECL1, and ECL2 of CXCR4-ED are thought to interact with the V3 loop, and accordingly peptides derived from these regions were synthesized and their anti-HIV-1 activity was evaluated to identify regions associated with anti-HIV-1 activity. An NT-fragment peptide, **N1** showed significant anti-HIV-1 activity. Cyclic peptides of ECL1 and ECL2, which mimic the structures of the native ECL1 and ECL2, showed higher anti-HIV-1 activity than the corresponding linear peptides. The **N1** peptide appears to bind to the V3 base and behave as an inhibitor of HIV-1 entry. Other candidates might be found based on ECL1 and ECL2 by

optimizing the appropriate cyclization. CXCR4-ED-derived peptidic inhibitors could be potent HIV-1 entry inhibitors, suppressing the emergence of drug resistant strains.

Experimental Section

Peptide synthesis: Peptides were synthesized by using the standard Fmoc solid-phase protocol, purified by RP-HPLC, and characterized by ToF-ESIMS. Detailed procedures and data are provided in the Supporting Information.

Biological assays: Anti-HIV-1 activity was assessed as protection against HIV-1 (NL4-3 strain)-induced cytopathogenicity in MT-4 cells. Mixtures of various concentrations of test peptide solutions and HIV-1 were added to MT-4 cells at a multiplicity of infection (MOI) of 0.001 and placed in a 96-well microplate. After a five-day incubation period at $37\,^\circ$C in a CO_2 incubator, the number of viable cells was determined using a 3-(4,5-dimethylthiazol-2-yl)-2,5-diphenyltetrazolium bromide (MTT) assay, and EC_{50} values were calculated. Cytotoxicity was determined based on the viability of mock-infected cells using the MTT method (CC_{50}). Each experiment was performed three times independently.

[1] F. Barre-Sinoussi, J. C. Chermann, F. Rey, M. T. Nugeyre, S. Chamaret, J. Gruest, C. Dauguet, C. Axler-Blin, F. Vézinet-Brun, C. Rouzioux, L. Montagnier, *Science* **1983**, *220*, 868–871.
[2] R. W. Doms, S. C. Peiper, *Virology* **1997**, *235*, 179–190.
[3] C. D. Rizzuto, R. Wyatt, N. Hernandez-Ramos, Y. Sun, P. D. Kwong, A. W. Hendrickson, J. Sodroski, *Science* **1998**, *280*, 1949–1953.
[4] G. Alkhatib, C. Combadiere, C. C. Broder, Y. Feng, P. E. Kennedy, P. M. Murphy, E. A. Berger, *Science* **1996**, *272*, 1955–1958.
[5] B. J. Doranz, J. Rucker, Y. Yi, R. J. Smyth, M. Samson, S. C. Peiper, M. Parmentier, R. G. Collman, R. W. Doms, *Cell* **1996**, *85*, 1149–1158.
[6] H. Deng, R. Liu, W. Ellmeier, S. Choe, D. Unutmaz, M. Burkhart, P. D. Marzio, S. Marmon, R. E. Sutton, C. M. Hill, C. B. Davis, S. C. Peiper, T. J. Schall, D. R. Littman, N. R. Landau, *Nature* **1996**, *381*, 661–666.
[7] T. Dragic, V. Litwin, G. P. Allaway, S. R. Martin, Y. Huang, K. A. Nagashima, C. Cayanan, P. J. Madon, R. A. Koup, J. P. Moore, W. A. Paxton, *Nature* **1996**, *381*, 667–673.
[8] Y. Feng, C. C. Broder, P. E. Kennedy, E. A. Berger, *Science* **1996**, *272*, 872–877.
[9] C. Hashimoto, T. Tanaka, T. Narumi, W. Nomura, H. Tamamura, *Expert Opin. Drug Discovery* **2011**, *6*, 1067–1090.
[10] D. K. Walker, S. Abel, P. Comby, G. J. Muirhead, A. N. Nedderman, D. A. Smith, *Drug Metab. Dispos.* **2005**, *33*, 587–595.
[11] H. Tamamura, Y. Xu, T. Hattori, X. Zhang, R. Arakaki, K. Kanbara, A. Omagari, A. Otaka, T. Ibuka, N. Yamamoto, H. Nakashima, N. Fujii, *Biochem. Biophys. Res. Commun.* **1998**, *253*, 877–882.
[12] N. Fujii, S. Oishi, K. Hiramatsu, T. Araki, S. Ueda, H. Tamamura, A. Otaka, S. Kusano, S. Terakubo, H. Nakashima, J. A. Broach, J. O. Trent, Z. X. Wang, S. C. Peiper, *Angew. Chem.* **2003**, *115*, 3373–3375; *Angew. Chem. Int. Ed.* **2003**, *42*, 3251–3253.
[13] E. De Clercq, N. Yamamoto, R. Pauwels, J. Balzarini, M. Witvrouw, K. De Vreese, Z. Debyser, B. Rosenwirth, P. Peichl, R. Datema, *Antimicrob. Agents Chemother.* **1994**, *38*, 668–674.
[14] D. Schols, S. Struyf, J. Van Damme, J. A. Este, G. Henson, E. De Clercq, *J. Exp. Med.* **1997**, *186*, 1383–1388.
[15] H. Tamamura, A. Ojida, T. Ogawa, H. Tsutsumi, H. Masuno, H. Nakashima, N. Yamamoto, I. Hamachi, N. Fujii, *J. Med. Chem.* **2006**, *49*, 3412–3415.
[16] T. Tanaka, T. Narumi, T. Ozaki, A. Sohma, N. Ohashi, C. Hashimoto, K. Itotani, W. Nomura, T. Murakami, N. Yamamoto, H. Tamamura, *ChemMedChem* **2011**, *6*, 834–839.
[17] K. Ichiyama, S. Yokoyama-Kumakura, Y. Tanaka, R. Tanaka, K. Hirose, K. Nannai, T. Edamatsu, M. Yanaka, Y. Niitani, N. Miyano-Kurosaki, H. Takaku, Y. Koyanagi, N. Yamamoto, *Proc. Natl. Acad. Sci. USA* **2003**, *100*, 4185–4190.
[18] G. C. Valks, G. McRobbie, E. A. Lewis, T. J. Hubin, T. M. Hunter, P. J. Sadler, C. Pannecouque, E. De Clercq, S. J. Archibald, *J. Med. Chem.* **2006**, *49*, 6162–6265.
[19] W. Zhan, Z. Liang, A. Zhu, S. Kurtkaya, H. Shim, J. P. Snyder, D. C. Liotta, *J. Med. Chem.* **2007**, *50*, 5655–5664.
[20] A. Khan, J. Nicholson, J. Greenman, L. Madden, G. McRobbie, C. Pannecouque, E. De Clercq, R. Ullom, D. L. Maples, R. D. Maples, J. D. Silversides, T. H. Hubin, S. J. Archibald, *J. Am. Chem. Soc.* **2009**, *131*, 3416–3417.
[21] G. J. Bridger, R. T. Skerlj, P. E. Hernandez-Abad, D. E. Bogucki, Z. Wang, Y. Zhou, S. Nan, E. M. Boehringer, T. Wilson, J. Crawford, M. Metz, S. Hatse, K. Princen, E. De Clercq, D. Schols, *J. Med. Chem.* **2010**, *53*, 1250–1260.
[22] R. T. Skerlj, G. J. Bridger, A. Kaller, E. J. McEachem, J. B. Crawford, Y. Zhou, B. Atsma, J. Langille, S. Nan, D. Veale, T. Wilson, C. Harwig, S. Haste, K. Princen, E. De Clercq, D. Schols, *J. Med. Chem.* **2010**, *53*, 3376–3388.
[23] I. Thordsen, S. Polzer, M. Schreiber, *BMC Infect. Dis.* **2002**, *2*, 31.
[24] K. Maeda, H. Nakata, Y. Koh, T. Miyakawa, H. Ogata, Y. Takaoka, S. Shibayama, K. Sagawa, D. Fukushima, J. Moravek, Y. Koyanagi, H. Mitsuya, *J. Virol.* **2004**, *78*, 8654–8662.
[25] P. R. Clapham, A. McKnight, *Br. Med. Bull.* **2001**, *58*, 43–59.
[26] A. Brelot, N. Heveker, M. Montes, M. Alizon, *J. Biol. Chem.* **2000**, *275*, 23736–23744.
[27] B. J. Doranz, *J. Virol.* **1999**, *73*, 2752–2761.
[28] S. Zolla-Pazner, T. Cardozo, *Nat. Rev. Immunol.* **2010**, *10*, 527–535.
[29] U. Neogi, S. B. Prarthana, G. D'Souza, A. DeCosta, V. S. Kuttiatt, U. Ranga, A. Shet, *AIDS Res. Ther.* **2010**, *7*, 24.
[30] N. H. Lin, C. Becerril, F. Giquel, V. Novitsky, J. Makhema, M. Essex, S. Lockman, D. R. Kuritzkes, M. Sagar, *Virology* **2012**, *433*, 296–307.
[31] T. Dragic, *J. Gen. Virol.* **2001**, *82*, 1807–1814.
[32] B. Wu, E. Y. Chien, C. D. Mol, G. Fenalti, W. Liu, V. Katritch, R. Abagyan, A. Brooun, P. Wells, F. C. Bi, D. J. Hamel, P. Kuhn, T. M. Handel, V. Cherezov, R. C. Stevens, *Science* **2010**, *330*, 1066–1071.
[33] M. Farzan, G. J. Babcock, N. Vasilieva, P. L. Wright, E. Kiprilov, T. Mirzabekov, H. Choe, *J. Biol. Chem.* **2002**, *277*, 29484–29489.
[34] C. T. Veldkamp, C. Seibert, F. C. Peterson, N. B. De La Cruz, J. C. Haugner III, H. Basnet, T. P. Sakmer, B. F. Volkman, *Sci. Signaling* **2008**, *1*, 1–9.
[35] K. Kitagawa, C. Aida, H. Fujiwara, T. Yagami, S. Futaki, M. Kogure, J. Ida, K. Inoue, *J. Org. Chem.* **2001**, *66*, 1–10.
[36] C. W. Hendrix, C. Flexner, R. T. MacFarland, C. Giandomenico, E. J. Fuchs, E. Redpath, G. Bridger, G. W. Henson, *Antimicrob. Agents Chemother.* **2000**, *44*, 1667–1673.
[37] C. Huang, S. N. Lam, P. Acharya, M. Tang, S. Xiang, S. S. Hussan, R. L. Stanfield, J. Robinson, J. Sodroski, I. A. Wilson, R. Wyatt, C. A. Bewley, P. D. Kwong, *Science* **2007**, *317*, 1930–1934.
[38] X. Sun, G. Cheng, M. Hao, J. Zheng, X. Zhou, J. Zhang, R. S. Taichman, K. J. Pienta, J. Wang, *Cancer Metastasis Rev.* **2010**, *29*, 709–722.
[39] A. Caruz, M. Samsom, J. M. Alonso, J. Alcami, F. Baleux, J. L. Virelizier, M. Parmentier, F. Arenzana-Seisdedos, *FEBS Lett.* **1998**, *426*, 271–278.
[40] C. C. Huang, M. Tang, M. Y. Zhang, S. Majeed, E. Montabana, R. L. Stanfield, D. S. Dimitrov, B. Korber, J. Sodroski, I. A. Wilson, R. Wyatt, P. D. Kwong, *Science* **2005**, *310*, 1025–1028.
[41] The PyMOL Molecular Graphics System, ver. 0.99rc6.

Cell-Permeable Stapled Peptides Based on HIV-1 Integrase Inhibitors Derived from HIV-1 Gene Products

Wataru Nomura,[†] Haruo Aikawa,[†] Nami Ohashi,[†] Emiko Urano,[‡] Mathieu Métifiot,[§] Masayuki Fujino,[‡] Kasthuraiah Maddali,[§] Taro Ozaki,[†] Ami Nozue,[†] Tetsuo Narumi,[†] Chie Hashimoto,[†] Tomohiro Tanaka,[†] Yves Pommier,[§] Naoki Yamamoto,[⊥] Jun A. Komano,[‡,∥] Tsutomu Murakami,[‡] and Hirokazu Tamamura*,[†]

[†]Department of Medicinal Chemistry, Institute of Biomaterials and Bioengineering, Tokyo Medical and Dental University, 2-3-10 Kandasurugadai, Chiyoda-ku, Tokyo 101-0062, Japan

[‡]AIDS Research Center, National Institute of Infectious Diseases, 1-23-1 Toyama, Shinjuku-ku, Tokyo 162-8640, Japan

[§]Laboratory of Molecular Pharmacology, Center for Cancer Research, National Cancer Institute, National Institutes of Health, Bethesda, Maryland 20892-4255, United States

[⊥]Department of Microbiology, Yong Loo Lin School of Medicine, National University of Singapore, Singapore 117597, Singapore

[∥]Department of Infectious Diseases, Osaka Prefectural Institute of Public Health, 1-3-69 Nakamichi, Higashinari-ku, Osaka 537-0025, Japan

◎ Supporting Information

ABSTRACT: HIV-1 integrase (IN) is an enzyme which is indispensable for the stable infection of host cells because it catalyzes the insertion of viral DNA into the genome and thus is an attractive target for the development of anti-HIV agents. Earlier, we found Vpr-derived peptides with inhibitory activity against HIV-1 IN. These Vpr-derived peptides are originally located in an α-helical region of the parent Vpr protein. Addition of an octa-arginyl group to the inhibitory peptides caused significant inhibition against HIV replication associated with an increase in cell permeability but also relatively high cytotoxicity. In the current study, stapled peptides, a new class

HIV-1 Vpr protein → Vpr-derived peptides → stapled peptide
• high helicity
• cell membrane permeability
• anti-HIV activity

of stabilized α-helical peptidomimetics were adopted to enhance the cell permeability of the above lead peptides. A series of stapled peptides, which have a hydrocarbon link formed by a ruthenium-catalyzed ring-closing metathesis reaction between successive turns of α-helix, were designed, synthesized, and evaluated for biological activity. In cell-based assays some of the stapled peptides showed potent anti-HIV activity comparable with that of the original octa-arginine-containing peptide (2) but with lower cytotoxicity. Fluorescent imaging experiments revealed that these stapled peptides are significantly cell permeable, and CD analysis showed they form α-helical structures, whereas the unstapled congeners form β-sheet structures. The application of this stapling strategy to Vpr-derived IN inhibitory peptides led to a remarkable increase in their potency in cells and a significant reduction of their cytotoxicity.
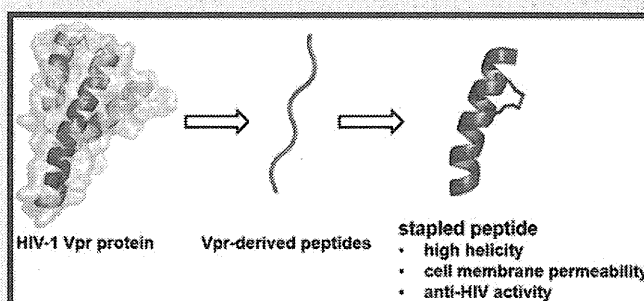
S everal antiretroviral drugs have been developed to date and are now available to treat human immunodeficiency virus type 1 (HIV-1) infection and acquired immunodeficiency syndrome (AIDS).[1] The main targets for antiretroviral drugs are viral enzymes such as protease, reverse transcriptase (RT) and integrase (IN) and surface proteins such as gp41 and coreceptors. New anti-HIV-1 drugs operating with different inhibitory mechanisms however, are required due to the emergence of viral strains with multidrug resistance (MDR), side effects and high costs of treatments. IN, an indispensable enzyme for the stable infection of the virus into host cells, catalyzes the insertion of viral DNA into the genome of host cells via strand transfer and 3′-end processing reactions. Thus, it is an attractive target for anti-HIV-1 drugs.[2,3] It has been assumed that during the transfer of viral DNA from cytoplasm to nucleus, the activity of IN must be negatively regulated to

prevent autointegration, which might abort the infection and we speculate that HIV must invoke a mechanism preventing the autointegration. The viral preintegration complex (PIC) contains viral nucleic acids; viral proteins such as RT, IN, capsids (p24[CA] and p7[NC]), matrix (p17[MA]), p6 and Vpr; cellular proteins HMG I (Y); and a barrier to autointegration factor (BAF).[4-7] Since these proteins exist in proximity in the PIC, they might physically and functionally interact with each other, and thus PIC components may regulate one another's function. An example of this is inhibition of IN activity by Vpr through its C-terminal domain.[8,9] In our previous study, the screening of an overlapping peptide library derived from HIV-1 proteins led

2235

to the identification of several peptide motifs with inhibitory activity against HIV-1 IN,[10] and the evaluation of effective inhibition of HIV-1 replication in cells using the identified peptide inhibitors possessing a cell membrane-permeable octa-arginine.[11] The original Vpr-fragment (1) and its octa-arginine-conjugate with cell membrane permeability (2) have been developed as lead peptides (Figure 1), which are located in the

1: Ac-EAIIRILQQLLFIHFRIG-NH$_2$
2: Ac-EAIIRILQQLLFIHFRIG-RRRRRRRR-NH$_2$

Figure 1. Amino acid sequences of peptides 1 and 2.

second helix region of the whole protein Vpr. In the structure–activity relationship studies, Glu-Lys pairs were introduced into the i and $i + 4$ positions to increase the helicity, and Ala-scan was also performed on the lead compound to identify the amino acid residues responsible for the inhibitory activity.[12] However, the addition of octa-arginine to these peptides led to an increase in cytotoxicity.

In the current study, hydrocarbon-stapled peptides, often utilized as a new class of stabilized α-helical peptidomimetics,[13–15] were adopted to enhance cell permeability in the above peptides, without octa-arginine (Figure 2). In stapled
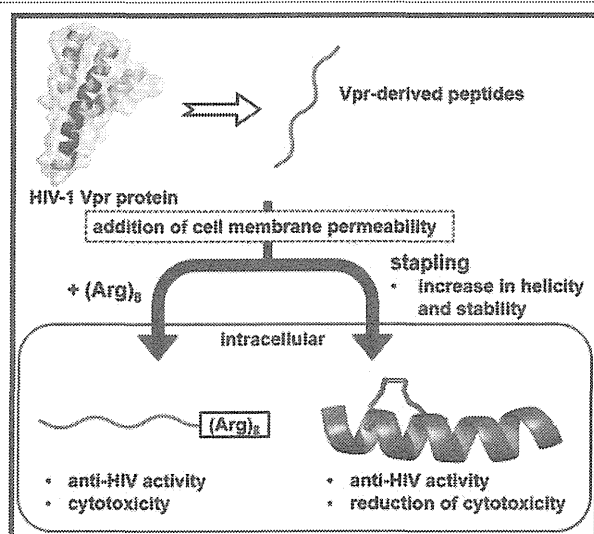

Figure 2. Outline of this study.

peptides, a ruthenium-catalyzed ring-closing metathesis (RCM) reaction between successive turns of α-helix causes formation of a hydrocarbon link.[16,17] Several stapled peptides were designed and synthesized, and their anti-HIV assay and bioimaging experiments using living cells were performed.
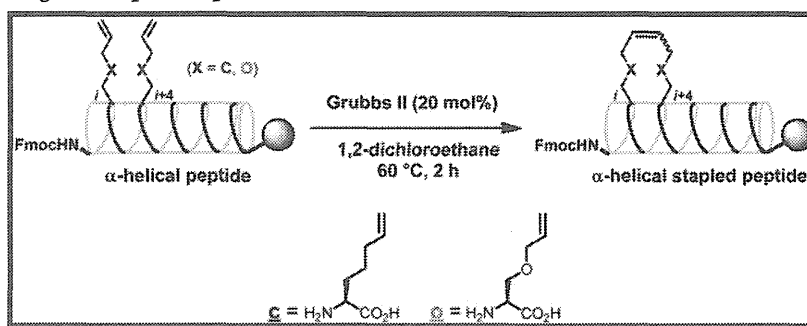
RESULTS AND DISCUSSION

Design and Synthesis of Stapled Peptides. The lead peptides 1 and 2 are shown in Figure 1.[10] It was found in our previous Ala-scan study that Phe[12], Ile[13], Phe[15], and Ile[17] are indispensable for IN inhibitory and anti-HIV activities.[12] Avoiding substitution for these residues, several stapled peptides cross-linked between the i and $i + 4$ positions were designed using all-hydrocarbon staple-type[18–20] and ether staple-type amino acid derivatives[21] (Table 1). Okamoto et al. reported that staple positioning was indeed important in binding of BimBH3 peptides to pro-survival proteins.[20] Protected linear peptides were constructed by Fmoc-solid

phase peptide synthesis on the Rink amide resin using Fmoc-protected all-hydrocarbon staple-type and ether staple-type amino acid derivatives (Scheme 1). The RCM reactions of the protected linear peptides were performed on the resin by treatment with 20 mol % of the ruthenium-mediated Grubbs second catalyst in 1,2-dichloroethane at 60 °C for 2 h. The RCM reactions of the all-hydrocarbon staple-types gave high yields (83–97%), while those of the ether staple-types did not cause adequate conversion ($\sim$0–57%), probably due to their instability or hydrophilicity. The yields of the conversion in the RCM reactions from linear to cyclic peptides are shown in Table 1. With peptides that have low conversion yields, it might be difficult for the two olefin moieties to interact each other and cross-link. The configuration of the double bonds was not determined.[22] After RCM, the Fmoc group at the N-terminus was removed, and the peptide was subsequently acetylated followed by the removal of the protecting groups and cleavage of the peptides from the resin using TFA. Purification of the crude peptides by preparative HPLC provided the stapled peptides as final products. In the synthesis of the corresponding linear peptides with olefinic side chains, the Fmoc group at the N-terminus was removed in the absence of RCM reactions, and the peptide was subsequently acetylated, the protecting groups were removed, and the peptide was cleaved from the resin using TFA and purified by HPLC. Since most of ether staple-type peptides had low conversion yields in the RCM reactions, only compounds 11S and 11L were synthesized. The conjugates of 6S with octa-arginine (17) and with the quartet repeat of arginine and glutamic acid (18), the conjugate of 6L with the quartet repeat of arginine and glutamic acid (19), and the conjugates of 6S with tetra-arginine (20), with penta-arginine (21), with hexa-arginine (22), and with hepta-arginine (23) were synthesized using the same method (Figure 5). For fluorescein-labeled peptides of 3S, 6S, 8S, 6L, 1, and 2, Fmoc-GABA-OH and fluorescein were condensed after the deprotection of the Fmoc group at the N-terminus (Supporting Information).

CD Spectroscopy of Linear and Stapled Peptides. The secondary structures of the synthetic peptides, stapled peptides, 3S–9S and 11S, and the linear peptides, 4L–6L, 8L, 9L, and 11L, were analyzed by CD spectroscopy (Figure 3). All of the stapled peptides, with the exception of 3S, showed double negative peaks at 208 and 222 nm, characteristic of an α-helical structure. In contrast, the corresponding linear peptides including compound 1 showed a broad negative peak around 215 nm, characteristic of a β-sheet structure. It is clear that stapling of the linear peptides causes a significant increase in α-helicity. Only one stapled peptide (3S) failed to show any sign of an α-helical structure, and consequently the corresponding linear peptide, 3L, was not used as a control.

Integrase (IN) Inhibition Assays of Stapled Peptides, 3S–9S and 11S, and Linear Peptides, 4L–6L, 8L, 9L, and 11L. The IN inhibitory activities of these compounds were evaluated *in vitro* by the 3′-end processing and strand transfer reactions (Table 2).[23–27] Compounds 4S, 5S, 6S, 6L, 8L, and 9L showed almost the same inhibitory levels as compound 1 in both the 3′-end processing and strand transfer reactions. Compounds 3S, 8S, 9S, 4L, 5L, and 11L showed 1.3–4.0-fold lower inhibitory activities than compound 1 in both 3′-end processing and strand transfer reactions. Compound 7S showed remarkably lower inhibitory potency against both activities. Compound 11S showed lower inhibitory activity on the 3′-end processing reaction than compound 1 but almost the same

Table 1. Sequences of Designed Stapled Peptides and Their Conversion Yields of RCM Reactions

| peptide	sequence	conversion [%][a]
3	Ac-cAIIcILQQLLFIHFRIG-NH₂	83
4	Ac-EcIIRcLQQLLFIHFRIG-NH₂	86
5	Ac-EAcIRIcQQLLFIHFRIG-NH₂	89
6	Ac-EAIcRILcQLLFIHFRIG-NH₂	85
7	Ac-EAIIcILQcLLFIHFRIG-NH₂	94
8	Ac-EAIIRcLQQcLFIHFRIG-NH₂	97
9	Ac-EAIIRIcQQLcFIHFRIG-NH₂	96
10	Ac-oAIIoILQQLLFIHFRIG-NH₂	19
11	Ac-EoIIRoLQQLLFIHFRIG-NH₂	57
12	Ac-EAoIRIoQQLLFIHFRIG-NH₂	50
13	Ac-EAIoRILoQLLFIHFRIG-NH₂	trace
14	Ac-EAIIoILQoLLFIHFRIG-NH₂	9
15	Ac-EAIIRoLQQoLFIHFRIG-NH₂	20
16	Ac-EAIIRIoQQLoFIHFRIG-NH₂	trace

[a]Determined by peak areas in reverse phase HPLC after deprotection and cleavage from resins.

Scheme 1
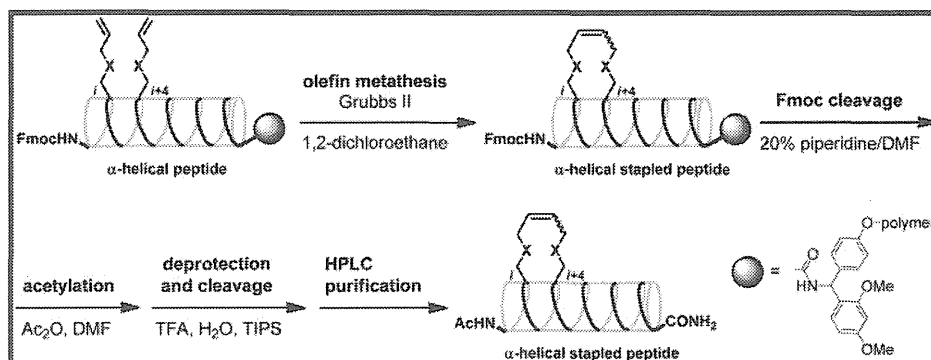
inhibitory level on the strand transfer reaction as that of compound 1. Compound 3S showed a β-sheet structure and low inhibitory activity, suggesting that stapling between 1 and 5 positions is not feasible and that the original amino acid residues Glu[1] and/or Arg[5] are indispensable for IN inhibitory activity. Compounds 4S and 5S retained the inhibitory activity of compound 1, while compounds 4L and 5L showed low inhibitory activity. These results suggest that stapling between the 2 and 6 positions and between the 3 and 7 positions is feasible, but the introduction of pentenyl moieties into the 2 and 6 positions or into the 3 and 7 positions is not. Maintenance of inhibitory activity at the level of that of compound 1 in both compounds 6S and 6L revealed that not only stapling between the 4 and 8 positions but also the

introduction of pentenyl moieties into the 4 and 8 positions is permissible. The original amino acid residue Ile[4] or Gln[8] is not essential for IN inhibitory activity. The considerable decrease in IN inhibitory activity of compound 7S showed that Arg[5] and Gln[9] are clearly important. The stapled peptide 7S showed no significant IN inhibitory activity, and consequently the corresponding linear peptide 7L was not synthesized. A decrease in activity of compounds 8S and 9S and maintenance in activity of compounds 8L and 9L suggest that Ile[6], Leu[7], Leu[10], or Leu[11] is not essential for IN inhibitory activity and that stapling by RCM between the 6 and 10 positions and between the 7 and 11 positions might have a disadvantageous effect on the other regions. A decrease in activity of compounds 11S and 11L suggests that the ether-type stapling is unsuitable,
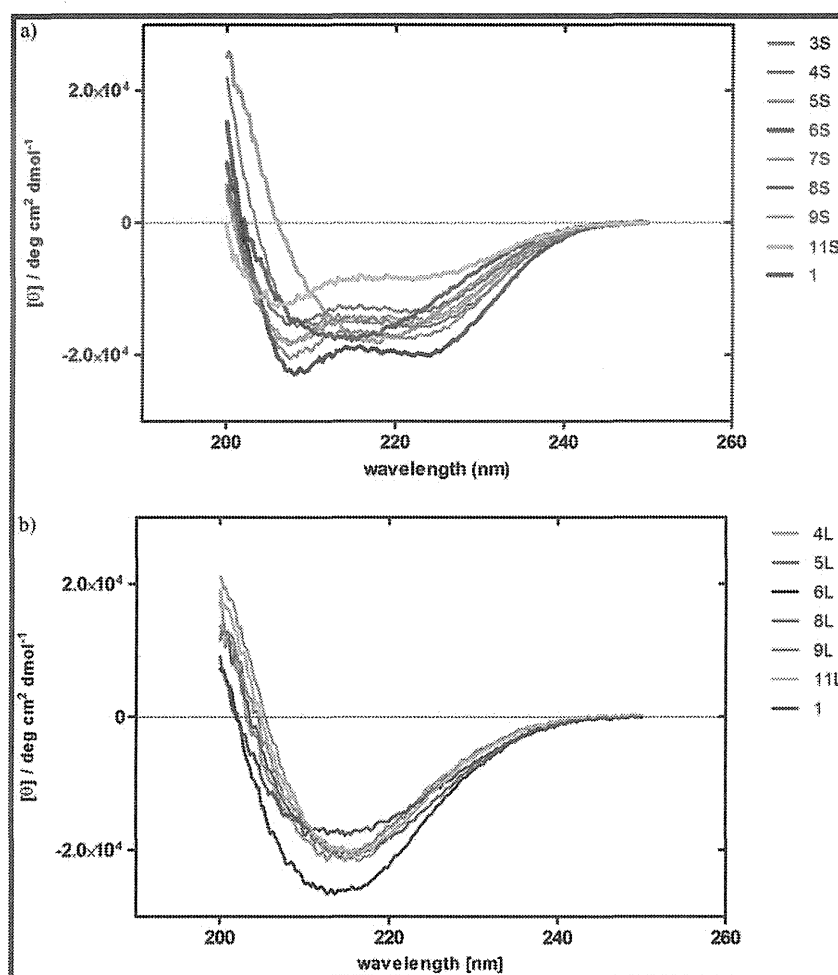
Figure 3. CD spectra of the stapled peptides 3S—9S, and 11S (a) and the linear peptides 4L–6L, 8L, 9L, and 11L (b) (12.5 μM) in H_2O containing 10% CH_3CN and 0.625% TFE at 20 °C.

Table 2. Inhibitory Activities (IC$_{50}$ Values) of the Stapled and Linear Peptides toward the 3'-End Processing and Strand Transfer Reactions Catalyzed by HIV-1 IN

peptide	IC$_{50}$ (μM)	
	3'-end processing	strand transfer
3S (stapled)	5.8 ± 0.8	3.8 ± 0.7
4S (stapled)	2.5 ± 0.4	1.1 ± 0.08
5S (stapled)	2.8 ± 0.3	1.2 ± 0.09
6S (stapled)	2.4 ± 0.4	0.84 ± 0.07
7S (stapled)	>111	54.4 ± 9.6
8S (stapled)	5.6 ± 0.7	4.1 ± 0.6
9S (stapled)	4.9 ± 0.6	1.9 ± 0.2
4L (linear)	5.2 ± 0.5	1.7 ± 0.3
5L (linear)	9.6 ± 0.6	4.4 ± 0.4
6L (linear)	2.6 ± 0.4	1.2 ± 0.09
8L (linear)	2.5 ± 0.3	1.0 ± 0.07
9L (linear)	2.1 ± 0.2	0.9 ± 0.06
11S (stapled)	4.2 ± 0.7	0.7 ± 0.08
11L (linear)	3.5 ± 0.3	1.7 ± 0.3
1	2.6 ± 0.2	1.1 ± 0.08
2	0.079 ± 0.007	0.036 ± 0.008

possibly because of hydrophilicity, while the reason why the inhibitory activity of 11S against the strand transfer reaction is retained is unclear. Compound 2 showed the highest inhibitory levels on both the 3'-end processing and strand transfer

reactions, which were approximately 30× higher than those of compound 1. The reason for this is not clear. The IN inhibition assays against the 3'-end processing and strand transfer reactions were performed *in vitro*, and thus, cell membrane permeability is not relevant.

MT-4 Luc Assays of Stapled Peptides, 3S–9S and 11S, and Linear Peptides, 4L–6L, 8L, 9L, and 11L. Anti-HIV activity of these compounds was assessed by an MT-4 Luc system, in which MT-4 cells were stably transduced with the firefly luciferase expression cassette by a murine leukemia viral vector.[28] MT-4 Luc cells constitutively express high levels of luciferase, but these high levels are significantly reduced by HIV-1 infection due to the high susceptibility of MT-4 cells to HIV-1 infection. Protection of MT-4 Luc cells from HIV-1-induced cell death maintains the luciferase signals at high levels. The cytotoxicity of test compounds can be evaluated by a decrease of luciferase signals in these MT-4 Luc systems. As reported previously, the parent compound (2) showed significant anti-HIV activity at concentrations above 2.5 μM (Figure 4).[10,12] Compound 1 showed no significant anti-HIV activity at concentrations below 10 μM, presumably due to lack of cell membrane permeability. Compound 6S showed significant anti-HIV activity at concentrations above 2.5 μM, its activity level being consistent with that of compound 2. Compound 8S at a concentration of 10 μM also showed significant anti-HIV activity. The corresponding linear peptides 6L and 8L did not show significant anti-HIV activity at
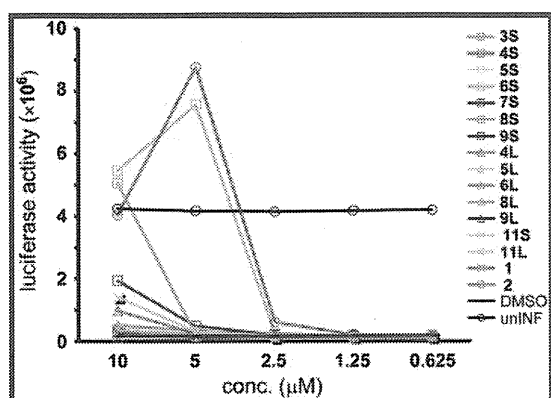
Figure 4. Luciferase signals in MT-4 Luc cells infected with HIV-1 in the presence of different concentrations of compounds 3S–9S, 4L–6L, 8L, 9L, 11S, and 11L. Luciferase activity is expressed as relative luciferase units (RLU). unINF: uninfected.

concentrations below 10 μM, suggesting that stapling was effective for both cell membrane permeability and the expression of activity inside cells with the result that HIV-1 replication was effectively inhibited. The other stapled peptides did not show significant anti-HIV activity at concentrations below 10 μM, possibly because of the introduction of the cross-link in inappropriate positions. All of the linear peptides failed to show significant anti-HIV activity, indicating that these peptides do not enter the cytoplasm or cannot access IN. Compounds 6S and 2 have almost the same level of anti-HIV activity in cells, although 2 has much higher IN inhibitory activity *in vitro* than compound 6S. The additional octa-arginine sequence might play a functional role besides influencing cell membrane permeability, and thus, conjugates of compounds 6S and 6L with hydrophilic sequences were synthesized to investigate the functional role of octa-arginine.

IN Inhibition Assays of Conjugates of Hydrophilic Sequence-containing Compounds 6S and 6L. As a comparative study of additional hydrophilic sequences, we investigated the functional role of octa-arginine with the conjugates of compounds 6S and 6L with the quartet repeat of arginine and glutamic acid (Figure 5, Table 3). Compound 17 showed high inhibitory levels with respect to both the 3′-end

processing and strand transfer reactions and its activity levels were comparable with those of compound 2. Compound 18 showed lower IN inhibitory levels, which were almost the same levels as those of compounds 19, 6S, and 1. It suggests that the addition of the quartet repeat of arginine and glutamic acid does not lead to an increase in IN inhibitory activities, and that the only addition of octa-arginine is effective.

Figure 5. Amino acid sequences of the conjugates of 6S with octa-arginine (17) and with the quartet repeat of arginine and glutamic acid (18), the conjugate of 6L with the quartet repeat of arginine and glutamic acid (19), and the conjugates of 6S with tetra-arginine (20), penta-arginine (21), hexa-arginine (22), and hepta-arginine (23). x = cross-linked all-hydrocarbon staple-type amino acid, z = 2-aminohept-6-enoic acid.

MT-4 Luc Assays of Conjugates of Compounds 6S and 6L with Hydrophilic Sequences.

Anti-HIV activity of these conjugates was assessed by the MT-4 Luc system (Figure 6). Compound 17 showed significant anti-HIV activity at concentrations above 1.25 μM but significant cytotoxicity at a concentration of 10 μM. Compound 18 showed significant anti-HIV activity at concentrations above 5 μM; its activity level was almost the same as that of compound 6S. Compound 19 showed significant anti-HIV activity at a concentration of 10 μM, whereas compound 6L did not show significant anti-HIV activity at concentrations below 10 μM. Thus the addition of the quartet repeat of arginine and glutamic acid results in a slight increase in anti-HIV activity in cells, but the increase was much lower than that resulting from the addition of octa-arginine. It is noteworthy that the octa-arginine addition has a possibility to cause cytotoxicity and also that stapled peptides have sufficient cell membrane permeability

Table 3. Inhibitory Activities (IC$_{50}$ Values) toward the 3′-End Processing and Strand Transfer Reactions Catalyzed by HIV-1 IN, DNA Binding Effects, anti-HIV Activities (EC$_{50}$ Values, p24, and MTT assays) and Cytotoxicities (CC$_{50}$ Values, MTT Assay) of the Peptides with Hydrophilic Sequences

peptide	IC$_{50}$ (μM) 3′-end processing	IC$_{50}$ (μM) strand transfer	DNA binding effect (μM)[a]	EC$_{50}$ (μM) p24 assay	EC$_{50}$ (μM) MTT assay	CC$_{50}$ (μM) MTT assay
17	0.14 ± 0.02	0.056 ± 0.011	4	4.29	3.08	7.04
18	1.47 ± 0.18	0.81 ± 0.13	37	9.56	6.81	>10
19	1.95 ± 0.25	1.13 ± 0.11	37	>10	>10	>10
6S	1.87 ± 0.14	0.71 ± 0.12	37	6.46	3.55	>10
6L	N.T.	N.T.	N.T.	>10	>10	>10
8S	N.T.	N.T.	N.T.	(14.22)	8.07	>10
8L	N.T.	N.T.	N.T.	>10	>10	>10
5S	2.6 ± 0.2	0.87 ± 0.14	37	>10	>10	>10
1	1.62 ± 0.26	1.34 ± 0.2	37	>10	>10	>10
2	0.119 ± 0.015	0.05 ± 0.004	4	3.51	4.54	5.91
AZT	N.T.	N.T.	N.T.	0.02	0.07	>100

[a]The lowest peptide concentrations that show retardation of DNA on wells of PAGE gels in integrase assays. That the same compounds give slightly different IC$_{50}$ values, as shown in Tables 2–4 can be explained by the fact that batches of compounds were tested at different times and that overlapping compounds were used to ensure the reproducibility of the assays.
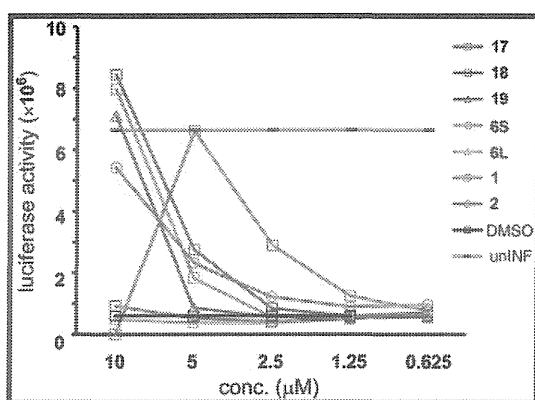
Figure 6. Luciferase signals in MT-4 Luc cells infected with HIV-1 in the presence of different concentrations of compounds 17, 18, and 19. Luciferase activity is expressed as relative luciferase units (RLU).

P24 ELISA and 3-(4,5-Dimethylthiazol-2-yl)-2,5-diphenyltetrazolium Bromide (MTT) Assays of Conjugates of Hydrophilic Sequence-Containing Compounds 6S and 6L.

The MT-4 Luc assay evaluates anti-HIV activity and cytotoxicity of compounds simultaneously: HIV-1-induced MT-4 cell death and compound-derived cell death both cause reduction of the luciferase signals, and consequently, anti-HIV activity and cytotoxicity of compounds cannot be distinguished by this assay system. The p24 ELISA and MTT assays of conjugates of compounds 6S and 6L with hydrophilic sequences were performed (Table 3). EC_{50} values in the p24 ELISA assay were based on the reduction of the HIV-1 p24 production in MT-4 cells infected with HIV-1 (NL4-3 strain). EC_{50} values in the MTT assay were based on the protection of HIV-1 (NL4-3 strain)-induced cytopathogenicity in MT-4 cells, and CC_{50} values in the MTT assay were based on the reduction of the viability of mock infected MT-4 cells. In these tests, compound 17 showed potent anti-HIV activity (EC_{50} (p24 assay) = 4.29 μM, EC_{50} (MTT assay) = 3.08 μM), but also significant cytotoxicity (CC_{50} = 7.04 μM). The anti-HIV activity of compound 18 (EC_{50} (p24 assay) = 9.56 μM, EC_{50} (MTT assay) = 6.81 μM) is lower than that of compound 17. This is consistent with the results in the MT-4 Luc assay (Figure 6). Compound 19 did not show significant anti-HIV activity at concentrations below 10 μM either in the p24 assay or in the MTT assay, but compound 19 showed significant but moderate anti-HIV activity at a concentration of 10 μM in the MT-4 Luc assay. Since MT-4 cells possess luciferase, background signals can be detected in the MT-4 Luc assay whose sensitivity compared to that of the more reliable p24 or MTT assays is not therefore refined. Consequently, compound 19 might have minimal or no anti-HIV activity. Compound 6S has potent anti-HIV activity (EC_{50} (p24 assay) = 6.46 μM, EC_{50} (MTT assay) = 3.55 μM), which is consistent with that of compound 17. The corresponding linear peptide 6L did not show significant anti-HIV activity at concentrations below 10 μM in either the p24 assay or in the MTT assay, indicating the effect of stapling. Compound 6S did not show significant cytotoxicity at concentrations below 10 μM in common with all the peptides lacking octa-arginine. Only compounds 17 and 2 showed potent cytotoxicity (CC_{50} = 7.04 μM, CC_{50} = 5.91 μM, respectively). The second most potent stapled peptide (8S) and its corresponding linear peptide (8L) showed a certain level of anti-HIV activity and almost no significant anti-HIV activity, respectively. These results are consistent with those in

the MT-4 Luc assay (Figures 4 and 6). Compound 5S, which did not show high anti-HIV activity in the MT-4 Luc assay, failed to exhibit significant anti-HIV activity at concentrations below 10 μM either in the p24 or the MTT assay. Compound 2 showed potent anti-HIV activity and cytotoxicity (EC_{50} (p24 assay) = 3.51 μM, EC_{50} (MTT assay) = 4.54 μM, CC_{50} = 5.91 μM), whereas compound 1 did not show significant anti-HIV activity or cytotoxicity at concentrations below 10 μM. These results are consistent with those from the MT-4 Luc assay. In the expression of anti-HIV activity in cells, stapling is therefore sufficient, and the addition of octa-arginine is not desirable because of cytotoxicity.
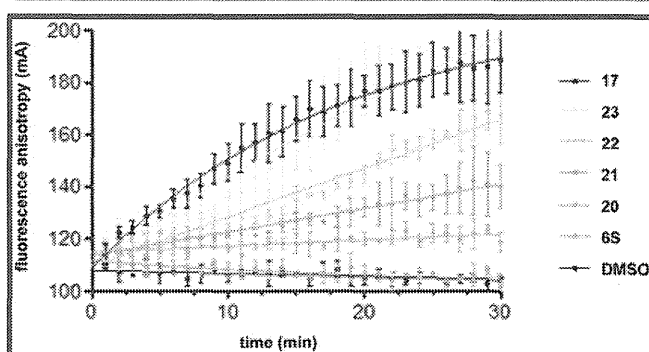
DNA Binding Effects of Conjugates of Compounds 6S and 6L with Hydrophilic Sequences.

In spite of the assay results obtained previously, the functional role of the additional octa-arginine sequence remains unclear. In the both the 3′-end processing and strand transfer reactions *in vitro*, the addition of the quartet repeat of arginine and glutamic acid failed to increase IN inhibitory activities, and only addition of octa-arginine was effective. Thus, the effects on DNA binding of conjugates of compounds 6S and 6L with hydrophilic sequences were investigated. Significant DNA binding effects were observed in the octa-arginine-containing peptides 17 and 2 at a concentration of 4 μM, whereas in the peptides with the quartet repeat of arginine and glutamic acid or lacking an additional sequence, DNA binding effects were observed at a concentration of 37 μM. This suggests that octa-arginine plays a critical role in DNA binding, perhaps because the arginine guanidino groups can bind to phosphonate groups of DNA and that the binding of peptides to the target DNA might lead to a significant increase in IN inhibitory activity.

IN Inhibition, P24 ELISA, MTT, and DNA Binding Assays of Conjugates of Compound 6S with Oligo-arginine Sequences.

The functional role of the additional octa-arginine sequence appears to be correlated to binding affinity for the target DNA and thus the IN inhibitory activities *in vitro*. The addition of the quartet repeat of arginine and glutamic acid appears not to have such a significant effect. This suggests that the hydrophilic nature of octa-arginine is not important but the sequential arginine sequence is critical. To investigate effects of the length of oligo-arginine sequences on DNA binding and IN inhibitory activities, the conjugates of compound 6S with tetra- (20), penta- (21), hexa- (22), and hepta-arginine (23) sequences were prepared (Figure 5). Compounds 20 and 21 showed 3–6× higher inhibition of both the 3′-end processing and strand transfer reactions than compound 6S (Table 4). Compound 22 showed 2× higher inhibitory levels than compounds 20 and 21 in both reactions. The activity levels of compound 23 were comparable with those of compound 17. Thus, the IN inhibitory activities appear to be positively correlated with the length of oligo-arginine sequences of the conjugates of compound 6S, and the addition of hepta-arginine is sufficient for increases in IN inhibitory activities. For DNA binding analysis, a fluorescent polarization assay was conducted. The interaction between the oligo-arginine and phosphates of DNA backbone should only be nonspecific electrostatic interactions. Although the changes in polarization did not reach equilibrium over the time-course examined, the differences in the rates of association of the peptides with DNA are positively correlated with the length of the oligo-arginine sequences of the conjugates of compound 6S (Figure 7). In the p24 ELISA and MTT assays, compounds 17 and 20–23 showed almost the same levels of anti-HIV activity

Table 4. Inhibitory Activities (IC$_{50}$ Values) toward the 3′-End Processing and Strand Transfer Reactions Catalyzed by HIV-1 IN, anti-HIV Activities (EC$_{50}$ Values, p24 and MTT Assays) and Cytotoxicities (CC$_{50}$ values, MTT Assay) of the Conjugates of Compound 6S with Oligo-arginine Sequences

peptide	IC$_{50}$ (μM) 3′-end processing	IC$_{50}$ (μM) strand transfer	EC$_{50}$ (μM) p24 assay	EC$_{50}$ (μM) MTT assay	CC$_{50}$ (μM) MTT assay
20	0.45 ± 0.02	0.22 ± 0.02	6.5	3.2	16
21	0.47 ± 0.03	0.21 ± 0.03	3.2	3.1	15
22	0.25 ± 0.01	0.14 ± 0.03	7.4	4.7	13
23	0.18 ± 0.01	0.062 ± 0.005	5.6	27% at 5 μM	12
17	0.17 ± 0.01	0.076 ± 0.009	7.1	28% at 5 μM	6.9
6S	2.6 ± 0.1	0.75 ± 0.08	8.3	6.4	>20
1	2.0 ± 0.2	2.2 ± 0.2	>20	N.T.	N.T.
2	0.16 ± 0.05	0.062 ± 0.009	6.4	N.T.	N.T.
AZT	N.T.	N.T.	0.29	0.07	>100

Figure 7. DNA binding properties of the conjugates of 6S with octa-arginine (17), with hepta-arginine (23), with hexa-arginine (22), with penta-arginine (21), and with tetra-arginine (20). Time courses at the 0.5 μM concentration of each peptide are presented. The oligonucleotide concentration is 10 nM.

(EC$_{50}$ = 3.1–7.4 μM), although exact EC$_{50}$ values of compounds 17 and 23 were not determined in the MTT assay because of the high cytotoxicity of the compounds. Cytotoxicity and the length of oligo-arginine sequences of the conjugates of compound 6S were inversely proportional to one another. Since compounds 20 and 21 with tetra- and penta-arginine sequences have sufficient IN inhibitory and DNA binding activities and relatively low cytotoxicity, these are useful leads in the series of stapled peptide-type IN inhibitors.
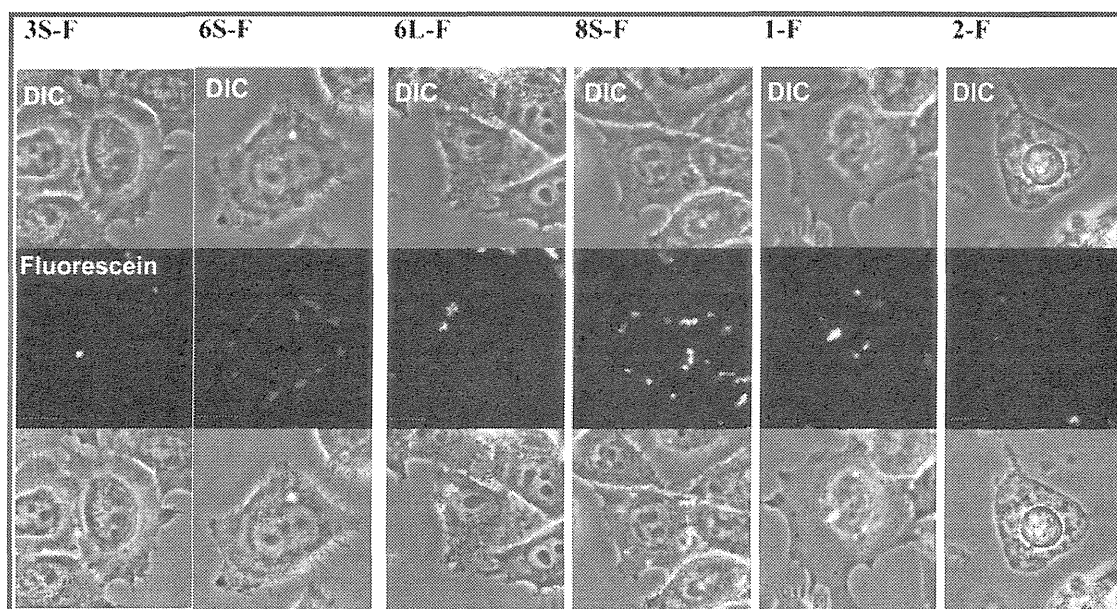
Stapled and Linear Peptides Labeled with Fluorescein: Imaging Experiments. To investigate whether stapled and linear peptides penetrate cell membranes, imaging experiments using peptides labeled with fluorescein were performed in HeLa cells (Figure 8). Compound 3S-F, the stapled peptide 3S labeled with fluorescein, was not observed inside cells, and it was concluded that compound 3S-F cannot penetrate cell membranes. According to the CD analysis, compound 3S does not form an α-helical structure (Figure 3) and thus is unable to penetrate cell membranes and did not show significant anti-HIV activity in the MT-4 Luc assay (Figure 4), although it showed significant IN inhibitory activity in vitro (Table 2). Cell membrane penetration of compound 6S-F, the stapled peptide 6S labeled with fluorescein, was observed, whereas cell membrane penetration of compound 6L-F, the linear peptide 6L labeled with fluorescein, was not. In

the image of 6L-F, the high accumulation of fluorescent dyes was observed on the cell surface. The phenomenon could suggest the aggregation of peptides. It is thought that, since compound 6S forms an α-helical structure, it can penetrate cell membranes and show potent anti-HIV activity, and since compound 6L does not form an α-helical structure, it cannot penetrate cell membranes and does not show significant anti-HIV activity. Compound 8S-F, the stapled peptide 8S labeled with fluorescein, showed imaging similar to that of compound 6S-F. Compound 8S forms an α-helical structure, can penetrate cell membranes and shows significant anti-HIV activity as in the case of compound 6S. However, in the case of compound 8S-F, the accumulation of fluorescent dyes on the cell surface was also observed. Compound 1-F, the peptide 1 labeled with fluorescein, was not observed inside cells, whereas compound 2-F, peptide 2 labeled with fluorescein, was observed inside cells. The addition to the structure of octa-arginine caused the peptide 1 to penetrate the cell membrane. The concentration of each peptide was 5 μM. In the MTT assay, the CC$_{50}$ value of peptide 2 was 5.91 μM (Table 3). It is possible that slightly rounded and no lamellipodia extensions of the cell image might be caused by the use of the peptide concentration similar to that of the CC$_{50}$ value. More cytotoxic effects might be detected if higher concentrations of the peptides were used. As a result, stapling (which can cause an increase in helicity) enhances cell membrane penetration. All the penetrating peptides (peptides 6S-F, 8S-F, and 2-F) in the cell showed localization in cytosol and accumulation near the cell membrane.

CONCLUSIONS

Stabilized α-helical peptidomimetics, stapled peptides, were applied to Vpr-derived fragments having HIV-1 IN inhibitory activity. Stapling of these lead compounds caused a significant increase in α-helicity and cell membrane penetration, and in the expression of potent anti-HIV activity in cells. The difference in the secondary structure of peptides did not make much difference in IN inhibitory activity. Even linear peptides might form α-helix structures when they bind to the target IN. Thus, the difference in the secondary structure might affect the difference in cell membrane penetration and thereby anti-HIV activity in cells. It is noteworthy that stapling and the addition of octa-arginine caused cell membrane penetration and that stapling did not involve cytotoxicity while incorporation of octa-arginine into the structures increased the cytotoxicity of the compounds. As a result, the stapled peptides 6S and 8S were found to be potent anti-HIV agents comparable with the original lead compound (2) containing octa-arginine. Adjustment of the length of additional oligo-arginine sequences of the stapled peptide 6S led to the development of compounds 20 and 21 with relatively high IN inhibitory activity and low cytotoxicity. The ratios of anti-HIV activity/cytotoxicity still might not be enough for drugs, but in the future the use of DNA binding units besides oligo-arginine sequences would resolve this drawback. The adoption of the stapled strategy to Vpr-derived peptides was successful, and these results might be useful for the further development of potent HIV-1 IN inhibitors. To date, several anti-HIV drugs have been reported, and their cocktail therapies using two or three drugs are known as highly active antiretroviral therapy (HAART), which has brought great success and hope in the clinical treatment of HIV-infected patients.[29] Recently, the first IN inhibitor, raltegravir (Merck),[2,3] has appeared in a clinical setting, and several inhibitors are under development. These IN inhibitors

Figure 8. Imaging experiments for cell permeability of the stapled and linear peptides labeled with fluorescein to HeLa cells. Each panel is divided into three sections as follows: upper, differential interference contrast (DIC) image; middle, fluorescein emission; lower, merged image. The peptide concentration is 5 μM. After addition of peptides, cells were incubated at 37 °C for 30 min under 5% CO_2 atmosphere. After washing three times with HBSS buffer, the fluorescent imaging was conducted by Fluoview FV10i confocal microscopy systems (Olympus). Orange bars in the panels represent 10 μm. The fluorescein-labeled peptides contain fluorescein–GABA instead of acetyl in the N-terminus.

might be useful in HAART. The present strategy, mimicking autoinhibition, would be less susceptible to resistance through mutation.

METHODS

Chemical synthesis and characterization methods for peptides and peptidomimetics are described in the Supporting Information.

CD Spectroscopy. CD measurements were performed on a JASCO J-820 spectropolarimeter equipped with thermoregulator (JASCO Corp., Ltd.), using 12.5 μM of peptides dissolved in 20% TFE water or 0.625% TFE water containing 10% CH_3CN. UV spectra were recorded at 20 °C in a quartz cell of 10.0 mm path length, a time constant of 0.25 s, and a 100 nm/min scanning speed with 0.2 nm resolution.

Integrase Assays. Recombinant IN was expressed in *E. coli* and purified as previously reported.[30] Integrase reactions were performed in 10 μL with 400 nM of recombinant IN, 20 nM of 5′-end [^{32}P]-labeled oligonucleotide substrate (full-length 21 nucleotide duplex)[30] and inhibitors or DMSO (drug solvent). Reaction mixtures were incubated at 37 °C (60 min) in buffer containing 50 mM MOPS, pH 7.2, 7.5 mM $MgCl_2$, and 14.3 mM 2-mercaptoethanol. Reactions were stopped by addition of 10 μL of loading dye (10 mM EDTA, 2% SDS, 95% deionized formamide, 0.025% xylene cyanol and 0.025% bromophenol blue). Reactions were then subjected to electrophoresis in 16% polyacrylamide–7 M urea gels. Gels were dried, and reaction products were visualized with a Typhoon 8600 (GE Healthcare, Little Chalfont, Buckinghamshire, UK). Densitometric analyses were performed using *ImageQuant* version 5.1 (Molecular Dynamics Inc.). Concentration of inhibitors allowing 50% reduction of enzyme activity (IC_{50}) and standard deviation (SD) were determined using *Prism* software version 5.0c (GraphPad Software, San Diego, CA) from at least three independent experiments.

Replication Assays. For MT-4 Luc assays, MT-4 Luc cells (2.5–5 $\times$ 10^3 cells) grown in 96-well plates were infected with HIV-1 NL4-3 ($\sim$50–250 pg) in the presence of varying concentrations of compounds. At 6–8 d postinfection, cells were lysed, and luciferase activity was measured using the Steady-Glo assay kits (Promega), according to the manufacture's protocol. Chemiluminescence was detected with a Veritas luminometer.

Anti-HIV-1 activity was determined by measuring the protection against HIV-1 (NL4-3 strain)-induced cytopathogenicity in MT-4 cells by the 3-(4,5-dimethylthiazol-2-yl)-2,5-diphenyltetrazolium bromide (MTT) assay or p24 (CA) concentrations in the culture supernatant by ELISA. Various concentrations of compounds were added to HIV-1-infected MT-4 cells at multiplicity of infection of 0.001 and placed in wells of a 96-well microplate. After 5 days' incubation at 37 °C in a CO_2 incubator, the number of viable cells was determined using the MTT method. Cytotoxicity of the compounds was determined by measurement of the reduction against the viability of mock-infected MT-4 cells. Levels of p24 antigen in the supernatants of 5-day cultures were also measured using a Retro TEK p24 antigen ELISA kit (ZeptroMetrix Corp., Buffalo, NY), according to the manufacture's protocol. Signals were detected using an ELx808 microplate photometer.

DNA Binding Effect (Table 3). Serial dilutions of peptides were mixed to IN and its radio-labeled DNA substrate in activity buffer (see Integrase Assays section). After 2 h at 37 °C, an equal volume of loading buffer (99% deionized formamide, 0.025% xylene cyanol, and 0.025% bromophenol blue) was added to the mixture. Samples were then loaded on 16% polyacrylamide–7 M urea gels. After 90 min migration at 2000 V, gels were dried, and migration of the DNA was visualized with a Typhoon 8600. The accumulation of signal in the well of the gel was visually investigated. The lowest concentration of peptides inducing complete retardation was reported.

DNA Binding Assays (Figure 7). A plate-based assay using fluorescence polarization was performed to monitor DNA binding. In this experiment, the integrase DNA substrate contains a fluorescein dye on its 3′-end (cleaved strand) and fluorescence anisotropy was monitored every min for 30 min at RT using the EnVision plate reader (Perkin-Elmer). Reactions were performed in absence of IN with 10 nM of fluorescent oligonucleotide and 0.5 μM peptide in buffer containing 0.1% BSA and 0.01% tween 20, 50 mM MOPS, pH 7.2, 7.5 mM $MgCl_2$, and 14.3 mM 2-mercaptoethanol. Each sample was assessed in triplicate, and a solution of 10% DMSO was used as control. Data analysis was done using *Prism* version 5.0c (GraphPad software).

■ ASSOCIATED CONTENT

ⓢ Supporting Information

Additional experimental procedures including MS data and figures: HPLC charts of final compounds. This material is available free of charge via the Internet at http://pubs.acs.org.

■ AUTHOR INFORMATION

Corresponding Author

*E-mail: tamamura.mr@tmd.ac.jp. Telephone: +81-3-5280-8036. Fax: +81-3-5280-8039.

Notes

The authors declare no competing financial interest.

■ ACKNOWLEDGMENTS

■ ABBREVIATIONS:

HIV, human immunodeficiency virus; AIDS, acquired immunodeficiency syndrome; RT, reverse transcriptase; IN, integrase; MDR, multidrug resistance; PIC, preintegration complex; BAF, barrier to autointegration factor; RCM, ring-closing metathesis; GABA, γ-aminobutyric acid; CD, circular dichroism; Luc, luciferase; ELISA, enzyme-linked immunosorbent assay; MTT, 3-(4,5-dimethylthial-2-yl)-2,5-diphenyltetrazalium bromide

■ REFERENCES

(1) Mitsuya, H., and Erickson, J. (1999) In Textbook of AIDS Medicine (Merigan, T. C., Bartlett, J. G., Bolognesi, D., Eds.), pp 751–780, Williams & Wilkins, Baltimore.

(2) Cahn, P., and Sued, O. (2007) Raltegravir: A New Antiretroviral Class for Salvage Therapy. Lancet 369, 1235–1236.

(3) Grinsztejn, B., Nguyen, B.-Y., Katlama, C., Gatell, J. M., Lazzarin, A., Vittecoq, D., Gonzalez, C. J., Chen, J., Harvey, C. M., and Isaacs, R. D. (2007) Safety and Efficacy of the HIV-1 Integrase Inhibitor Raltegravir (MK-0518) in Treatment-Experienced Patients with Multidrug-Resistant Virus: A Phase II Randomised Controlled Trial. Lancet 369, 1261–1269.

(4) Bukrinsky, M. I., Haggerty, S., Dempsey, M. P., Sharova, N., Adzhubei, A., Spitz, L., Lewis, P., Goldfarb, D., Emerman, M., and Stevenson, M. (1993) A Nuclear-Localization Signal within HIV-1 Matrix Protein That Governs Infection of Nondividing Cells. Nature 365, 666–669.

(5) Miller, M. D., Farnet, C. M., and Bushman, F. D. (1997) Human Immunodeficiency Virus Type 1 Preintegration Complexes: Studies of Organization and Composition. J. Virol. 71, 5382–5390.

(6) Farnet, C. M., and Bushman, F. D. (1997) HIV-1 cDNA Integration: Requirement of HMG I(Y) Protein for Function of Preintegration Complexes in Vitro. Cell 88, 483–492.

(7) Chen, H., and Engelman, A. (1998) The Barrier-to-Autointegration Protein Is a Host Factor for HIV Type 1 Integration. Proc. Natl. Acad. Sci. U.S.A. 95, 15270–15274.

(8) Gleenberg, I. O., Herschhorn, A., and Hizi, A. (2007) Inhibition of the Activities of Reverse Transcriptase and Integrase of Human Immunodeficiency Virus Type-1 by Peptides Derived from the Homologous Viral Protein R (Vpr). J. Mol. Biol. 369, 1230–1243.

(9) Bischerour, J., Tauc, P., Leh, H., De Rocquigny, H., Roques, B., and Mouscadet, J. F. (2003) The (52–96) C-Terminal Domain of Vpr Stimulates HIV-1 IN-Mediated Homologous Strand Transfer of Miniviral DNA. Nucleic Acids Res. 31, 2694–2702.

(10) Suzuki, S., Urano, E., Hashimoto, C., Tsutsumi, H., Nakahara, T., Tanaka, T., Nakanishi, Y., Maddali, K., Han, Y., Hamatake, M., Miyauchi, K., Pommier, Y., Beutler, J. A., Sugiura, W., Fuji, H., Hoshino, T., Itotani, K., Nomura, W., Narumi, T., Yamamoto, N., Komano, J. A., and Tamamura, H. (2010) Peptide HIV-1 Integrase Inhibitors from HIV-1 Gene Products. J. Med. Chem. 53, 5356–5360.

(11) Suzuki, T., Futaki, S., Niwa, M., Tanaka, S., Ueda, K., and Sugiura, Y. (2002) Possible Existence of Common Internalization Mechanisms among Arginine-Rich Peptides. J. Biol. Chem. 277, 2437–2443.

(12) Suzuki, S., Maddali, K., Hashimoto, C., Urano, E., Ohashi, N., Tanaka, T., Ozaki, T., Arai, H., Tsutsumi, H., Narumi, T., Nomura, W., Yamamoto, N., Pommier, Y., Komano, J. A., and Tamamura, H. (2010) Peptidic HIV Integrase Inhibitors Derived from HIV Gene Products: Structure-Activity Relationship Studies. Bioorg. Med. Chem. 18, 6771–6775.

(13) Schafmeister, C. E., Po, J., and Verdine, G. L. (2000) An All-Hydrocarbon Cross-Linking System for Enhancing the Helicity and Metabolic Stability of Peptides. J. Am. Chem. Soc. 122, 5891–5892.

(14) Zhang, H., Zhao, Q., Bhattacharya, S., Waheed, A. A., Tong, X., Hong, A., Heck, S., Curreli, F., Goger, M., Cowburn, D., Freed, E. O., and Debnath, A. K. (2008) A Cell-Penetrating Helical Peptide as a Potential HIV-1 Inhibitor. J. Mol. Biol. 378, 565–580.

(15) Verdine, G. L., and Hilinski, G. J. (2012) In Methods in Enzymology (Wittrup, K. D., Verdine, G. L., Eds.), Vol 503, pp 3–31, Elsevier Inc., Amsterdam.

(16) Blackwell, H. E., and Grubbs, R. H. (1998) Highly Efficient Synthesis of Covalently Cross-Linked Peptide Helices by Ring-Closing Metathesis. Angew. Chem., Int. Ed. 37, 3281–3284.

(17) Chatterjee, A. K., Choi, T.-L., Sanders, D. P., and Grubbs, R. H. (2003) A General Model for Selectivity in Olefin Cross Metathesis. J. Am. Chem. Soc. 125, 11360–11370.

(18) Hung, K., Harris, P. W. R., and Brimble, M. A. (2010) Synthesis of Methyl N-Boc-(2S,4R)-4-methylpipecolate. J. Org. Chem. 75, 8728–8731.

(19) Bautista, A. D., Appelbaum, J. S., Craig, C. J., Michel, J., and Schepartz, A. (2010) Bridged β^3-Peptide Inhibitors of p53–hDM2 Complexation: Correlation between Affinity and Cell Permeability. J. Am. Chem. Soc. 132, 2904–2906.

(20) Okamoto, T., Zobel, K., Fedorova, A., Quan, C., Yang, H., Fairbrother, W. J., Huang, D. C. S., Smith, B. J., Deshayes, K., and Czabotar, P. E. (2013) Stabilizing the Pro-Apoptotic BimBH3 Helix (BimSAHB) Does Not Necessarily Enhance Affinity or Biological Activity. ACS Chem. Biol. 8, 297–302.

(21) Boal, A. K., Guryanov, I., Moretto, A., Crisma, M., Lanni, E. L., Toniolo, C., Grubbs, R. H., and O'Leary, D. J. (2007) Facile and E-Selective Intramolecular Ring-Closing Metathesis Reactions in 3_{10}-Helical Peptides: A 3D Structural Study. J. Am. Chem. Soc. 129, 6986–6987.

(22) Kim, Y.-W., Grossmann, T. N., and Verdine, G. L. (2011) Synthesis of All-Hydrocarbon Stapled α-Helical Peptides by Ring-Closing Olefin Metathesis. Nat. Protoc. 6, 761–771.

(23) Yan, H., Mizutani, T. C., Nomura, N., Tanaka, T., Kitamura, Y., Miura, H., Nishizawa, M., Tatsumi, M., Yamamoto, N., and Sugiura, W. (2005) A Novel Small Molecular Weight Compound with a Carbazole Structure That Demonstrates Potent Human Immunodeficiency Virus Type-1 Integrase Inhibitory Activity. Antivir. Chem. Chemother. 16, 363–373.

(24) Marchand, C., Zhang, X., Pais, G. C. G., Cowansage, K., Neamati, N., Burke, T. R., Jr., and Pommier, Y. (2002) Structural Determinants for HIV-1 Integrase Inhibition by β-Diketo Acids. J. Biol. Chem. 277, 12596–12603.

(25) Semenova, E. A., Johnson, A. A., Marchand, C., Davis, D. A., Tarchoan, R., and Pommier, Y. (2006) Preferential Inhibition of the

Magnesium-Dependent Strand Transfer Reaction of HIV-1 Integrase by α-Hydroxytropolones. *Mol. Pharmacol. 69*, 1454–1460.

(26) Leh, H., Brodin, P., Bischerour, J., Deprez, E., Tauc, P., Brochon, J. C., LeCam, E., Coulaud, D., Auclair, C., and Mouscadet, J. F. (2000) Determinants of Mg^{2+}-Dependent Activities of Recombinant Human Immunodeficiency Virus Type 1 Integrase. *Biochemistry 39*, 9285–9294.

(27) Marchand, C., Neamati, N., and Pommier, Y. (2001) In Vitro Human Immunodeficiency Virus Type 1 Integrase Assays. In *Methods in Enzymology (Drug-Nucleic Acid Interactions)* (Chaires, J. B., Waring, M. J., Eds.), Vol 340, pp 624–633, Elsevier Inc., Amsterdam.

(28) Hazen, R. J., Harvey, R. J., St. Clair, M. H., Ferris, R. G., Freeman, G. A., Tidwell, J. H., Schaller, L. T., Cowan, J. R., Short, S. A., Romines, K. R., Chan, J. H., and Boone, L. R. (2005) Anti-Human Immunodeficiency Virus Type 1 Activity of the Nonnucleoside Reverse Transcriptase Inhibitor GW678248 in Combination with Other Antiretrovirals against Clinical Isolate Viruses and in Vitro Selection for Resistance. *Antimicrob. Agents Chemother. 49*, 4465–4473.

(29) Hashimoto, C., Tanaka, T., Narumi, T., Nomura, W., and Tamamura, H. (2011) The Success and Failures of HIV Drug Discovery. *Expert Opin. Drug Discovery 6*, 1067–1090.

(30) Métifiot, M., Maddali, K., Naumova, A., Zhang, X., Marchand, C., and Pommier, Y. (2010) Biochemical and Pharmacological Analyses of HIV-1 Integrase Flexible Loop Mutants Resistant to Raltegravir. *Biochemistry 49*, 3715–3722.

Low-Molecular-Weight CXCR4 Ligands with Variable Spacers

Tetsuo Narumi,[a] Haruo Aikawa,[a] Tomohiro Tanaka,[a] Chie Hashimoto,[a] Nami Ohashi,[a] Wataru Nomura,[a] Takuya Kobayakawa,[a] Hikaru Takano,[a] Yuki Hirota,[a] Tsutomu Murakami,[b] Naoki Yamamoto,[c] and Hirokazu Tamamura*[a]

Low-molecular-weight CXCR4 ligands based on known lead compounds including the 14-mer peptide T140, the cyclic pentapeptide FC131, peptide mimetics, and dipicolylamine-containing compounds were designed and synthesized. Three types of aromatic spacers, 1,4-phenylenedimethanamine, naphthalene-2,6-diyldimethanamine, and [1,1'-biphenyl]-4,4'-diyldimethanamine, were used to build four pharmacophore groups. As pharmacophore groups, 2-pyridylmethyl and 1-naphthylmethyl are present in all of the compounds, and several aromatic groups and a cationic group from 1-propylguanidine and 1,1,3,3-tetramethyl-2-propylguanidine were also used. Several compounds showed significant CXCR4 binding affinity, and zinc(II) complexation of bis(pyridin-2-ylmethyl)amine moieties resulted in a remarkable increase in CXCR4 binding affinity.

Introduction

CXCR4 is a chemokine receptor that transduces signals of its endogenous ligand, CXCL12/stromal cell-derived factor-1 (SDF-1).[1–4] This receptor is a member of the seven-transmembrane GPCR family, and has been reported to exist and function as an oligomer,[5] which was elucidated by our molecular ruler approach.[6] The CXCR4–CXCL12 axis plays a physiological role in embryonic stages in chemotaxis,[7] angiogenesis,[8,9] and neurogenesis.[10,11] CXCR4 is associated with many disorders including cancer cell metastasis,[12–14] leukemia cell progression,[15,16] HIV infection/AIDS,[17,18] and rheumatoid arthritis;[19,20] it is therefore a major target in the discovery of chemotherapeutic treatments for these diseases. To date, many researchers, including ourselves, have developed potent CXCR4 antagonists. A 14-mer peptide, T140, and a cyclic pentapeptide, FC131, have been found to be potent CXCR4 antagonists.[21–27] In addition, downsizing of these peptides has led to the de-

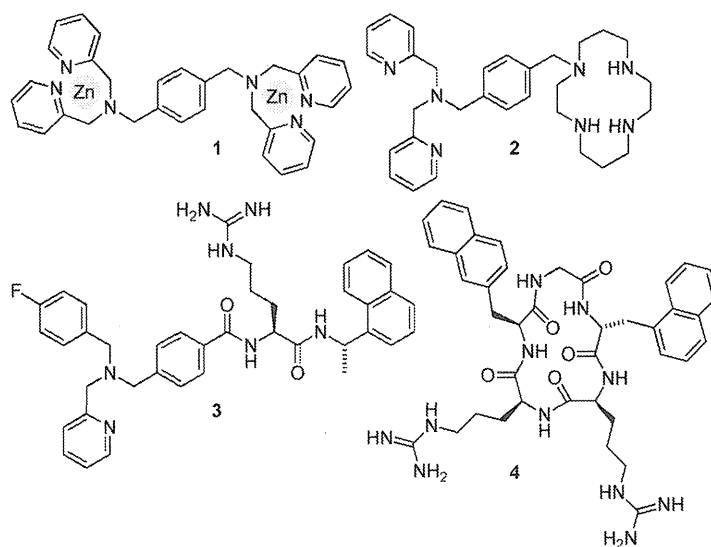Figure 1. Reported low-molecular-weight CXCR4 antagonists.

velopment of active small-molecular peptide mimetics.[28] Another peptide mimetic, KRH-1636,[29] and a bicyclam, AMD3100,[30,31] have also been reported. Furthermore, several compounds based on monocyclams[32] and noncyclams[33,34] have been reported. Other aza-macrocyclic compounds such as the Dpa–Zn complex 1[35] and the Dpa–cyclam compound 2[36] have been developed as non-peptide leads (Figure 1). These lead compounds have 1,4-phenylenedimethanamine structures with amino groups presenting basic/aromatic moieties. We recently developed small-molecular peptide mimetics containing benzyl and 2-pyridylmethyl amino groups, such as compound 3[37] and cyclic pentapeptide FC131 derivatives containing two naphthalene moieties (e.g., 4).[38] In the study presented herein, we tried to develop more effective small mole-

[a] Dr. T. Narumi, Dr. H. Aikawa, Dr. T. Tanaka, C. Hashimoto, Dr. N. Ohashi, Dr. W. Nomura, T. Kobayakawa, H. Takano, Y. Hirota, Prof. H. Tamamura
Institute of Biomaterials and Bioengineering
Tokyo Medical and Dental University
2-3-10 Kandasurugadai, Chiyoda-ku, Tokyo 101-0062 (Japan)
E-mail: tamamura.mr@tmd.ac.jp

[b] Dr. T. Murakami
AIDS Research Center, National Institute of Infectious Diseases
1-23-1 Toyama, Shinjuku-ku, Tokyo 162-8640 (Japan)

[c] Prof. N. Yamamoto
Department of Microbiology, Yong Loo Lin School of Medicine
National University of Singapore
Block MD4, 5 Science Drive 2, Singapore 117597 (Singapore)